# *Toxoplasma* GRA15 and GRA24 are important activators of the host innate immune response in the absence of TLR11

**Debanjan Mukhopadhyay[1], David Arranz-Solís[1], Jeroen P.J. Saeij[1*]**

[1]Department of Pathology, Microbiology and Immunology, University of California Davis, Davis, California, United States of America

**Running title:** GRA15 and GRA24 activate the immune response in TLR11-deficient hosts

**Key words: GRA15, GRA24, NFκB, p38 MAPK, TLR11, *Toxoplasma*, Toxoplasmosis**

## Abstract

The murine innate immune response against *Toxoplasma gondii* is predominated by the interaction of TLR11/12 with *Toxoplasma* profilin. However, mice lacking *Tlr11* or humans, who do not have functional TLR11 or TLR12, still elicit a strong innate immune response upon *Toxoplasma* infection. The parasite factors that determine this immune response are largely unknown. Herein, we investigated two dense granule proteins (GRAs) secreted by *Toxoplasma,* GRA15 and GRA24*,* for their role in stimulating the innate immune response in *Tlr11*$^{-/-}$ mice and in human cells, which naturally lack TLR11/TLR12. Our results show that GRA15 and GRA24 synergistically shape the early

immune response and parasite virulence in *Tlr11*$^{-/-}$ mice, with GRA15 as the predominant effector. Nevertheless, acute virulence in *Tlr11*$^{-/-}$ mice is still dominated by allelic combinations of *ROP18* and *ROP5*, which are effectors that determine evasion of the immunity-related GTPases. In human macrophages, GRA15 and GRA24 play a major role in the induction of IL12, IL18 and IL1β secretion. We further show that GRA15/GRA24-mediated IL12, IL18 and IL1β secretion activates IFNγ secretion by peripheral blood mononuclear cells (PBMCs), which controls *Toxoplasma* proliferation. Taken together, our study demonstrates the important role of GRA15 and GRA24 in activating the innate immune response in hosts lacking TLR11.

## Importance

In mice, the early immune response against *Toxoplasma* is dominated by TLR11-mediated release of IL-12, which subsequently induces protective IFNγ. Here we show that in *Tlr11*$^{-/-}$ mice and in human cells, which do not have TLR11, the *Toxoplasma* GRA15 and GRA24 effectors play an important role in induction of IL12, IL18 and IL1β, and thus in the subsequent protective IFNγ secretion.

## Introduction

*Toxoplasma gondii* is an obligate intracellular parasite capable of infecting any nucleated cell of any warm-blooded animal, including humans. It can cause lifelong persistent infections by forming semi-dormant cysts in muscles and the brain (1–3). *Toxoplasma* resides within a non-fusogenic vacuole called the parasitophorous vacuole

(PV), which is separated from the host cell cytosol by the PV membrane (PVM), preventing the parasite from being recognized by the host innate immune system. However, the cytokine interferon-gamma (IFNγ) activates effector mechanisms that can mediate the elimination of *Toxoplasma*. Inflammatory cytokines produced by macrophages and dendritic cells (DCs) in response to Toll-like receptor (TLR) recognition of conserved pathogen associated molecular patterns (PAMPs) are important for subsequent production of IFNγ. For example, in mice the *Toxoplasma* actin-binding protein profilin is recognized by a heterodimer of TLR11/12 that is located in the endosome, inducing a signaling cascade leading to the production of interleukin (IL)12 by DCs (4–6). IL12 in turn activates Natural Killer (NK) and T cells to secrete IFNγ, which can trigger a variety of toxoplasmacidal mechanisms (7, 8). In mice, IFNγ-induced immunity related GTPases (IRGs) that can coat and vesiculate the PVM, and ultimately destroy the parasite inside, play a dominant role in resistance to *Toxoplasma* (9–11).

Innate immunity can also be activated by specific cytosolic receptors (often nucleotide-binding domain and leucine-rich repeat-containing receptors or NLRs) as a part of a multi-protein complex called the inflammasome (12). In mice, *Toxoplasma* can activate the NLRP1 and NLRP3 inflammasomes (13), leading to IL1β/IL18 production, which together with IL12 can enhance IFNγ secretion and thereby contribute to host resistance against *Toxoplasma* (14, 15). However, inflammasome activation in *Tlr11*$^{-/-}$ mice can also induce a pathological inflammatory response (16).

Human sensing and killing of *Toxoplasma* differs from mice, as humans lack functional TLR11/12 and do not have IRGs (17). It was recently shown that the alarmin

S100A11 secreted from infected monocytes or fibroblasts can shape the human immune response through secretion of the chemokine ligand 2 (CCL2) (18). In addition, cytosolic recognition of *Toxoplasma* in human monocytes was shown to partly rely on the NLRP1 and NLRP3 inflammasome, resulting in secretion of IL1β (19, 20). Furthermore, guanylate binding protein (GBP)1 facilitates disruption of the PV in IFNγ-stimulated human macrophages, which causes release of parasite nucleic acids that can activate cytosolic absent in melanoma 2 (AIM2) and caspase 8-dependent apoptosis (21). This could be another potential route of immune activation as recognition of cytosolic nucleic acids induces the type I interferon pathway.

*Toxoplasma* can counteract the host immune response by secreting effector proteins, ROPs and GRAs, into the host cell from specialized secretory organelles called rhoptries and dense granules, respectively (22, 23). In Europe and North America, strains belonging to four different *Toxoplasma* clonal lineages (types I, II, III and XII) are commonly isolated in animals and humans, although most infections are caused by type II strains (24–26). In mice, strain differences in virulence and modulation of host cell signaling are largely due to polymorphisms in ROPs and GRAs. For example, ROP18 (a secreted kinase) and ROP5 (a pseudokinase) determine strain differences in virulence in mice by cooperatively blocking the IFNγ-induced IRGs (10, 27–29). Several GRA proteins are localized on the PVM and can modulate the host immune response (30–32). For instance, GRA15 from type II strains activates the NFκB pathway, leading to macrophage production of inflammatory cytokines such as IL12 and IL1β (31, 33). Other GRAs are secreted beyond the PVM, where they can modulate host cell signaling pathways (22, 34–36). For example, GRA24 binds to p38α MAPK

leading to its autophosphorylation and constitutive activation (35). Together, GRA15 and GRA24 drive the classical activation of macrophages (M1) via the activation of NFκB and p38 MAPK (35, 37, 38). By contrast, the polymorphic kinase ROP16 from type I and type III strains drives the alternative activation of macrophages (M2) via the phosphorylation of the STAT6 and STAT3 transcription factors (37, 39, 40). It is likely that the deliberate activation of the immune response by *Toxoplasma* effectors is a strategy to limit its virulence thereby promoting the survival of its host and the formation of tissue cysts, which are the only stages in the intermediate host that are orally infectious.

Given the large impact of GRA15 and GRA24 on macrophage gene expression and production of IL12 and IL1β, it seems surprising that their *in vivo* effect on parasite virulence is relatively minor (31, 35). Mice infected with type II Δ*gra15* or Δ*gra24* parasites had elevated parasite numbers early after infection, but as the infection progressed, parasite burden and host susceptibility were no different from those following wild-type type II strain infections (31, 35, 41). Increased type II Δ*gra15* early parasite burdens were associated with decreased IL12 and IFNγ levels 2 days after infection (31). Similar results were obtained after infection of mice with the Δ*gra24* strain (35). Possibly, the effects of GRA15 and GRA24 in these studies were masked by profilin: as the infection progresses and parasites lyse out of host cells, PAMPS, such as profilin, are released and activate TLR11/12. At this stage, IL12/IL1β and subsequent IFNγ production are probably no longer dependent on GRA15 and GRA24. However, humans and many animals do not have functional TLR11/12 or IFNγ-inducible IRGs (17), and therefore *Toxoplasma* virulence of a particular strain in mice might not

116 correlate with virulence in other species. In *Tlr11*$^{-/-}$ mice, neutrophils are the main
117 producers of IFNγ with a minor role of NK and T cells (42). The production of IFNγ by
118 neutrophils is dependent on IL1β and TNFα, but not on IL12 (42). In addition, IL18
119 secreted upon inflammasome activation plays a key role in the IFNγ response from
120 CD4$^{+}$ T cells and the subsequent disease outcome in *Tlr11*$^{-/-}$ mice (43). Thus, GRA15
121 and GRA24, by inducing IL1β, IL18, TNFα and IL12, might play an important role in the
122 production of IFNγ in hosts lacking TLR11. Herein, we tested this hypothesis by
123 infecting *Tlr11*$^{-/-}$ mice with wild-type, Δ*gra15*, Δ*gra24* and Δ*gra15/24* parasites. Our data
124 indicate that although parasites that do not express GRA15 and/or GRA24 induced
125 significantly less inflammatory cytokines, a significant increase in virulence compared to
126 wild-type was only observed after subcutaneous infection, likely because *Tlr11*$^{-/-}$ mice
127 were already extremely susceptible to wild-type *Toxoplasma* infections. We further
128 show that in *Tlr11*$^{-/-}$ mice IRG-mediated killing of *Toxoplasma* is likely still the major
129 mechanism of resistance, as parasites that express avirulent ROP5 and ROP18 were
130 completely avirulent in these mice. In human THP1-derived macrophages and PBMCs,
131 GRA15 and GRA24 determined the induction of inflammatory cytokines and thereby
132 had a large effect on parasite proliferation. Thus, in the absence of TLR11, GRA15 and
133 GRA24 are the major parasite effectors that activate the innate immune response and it
134 is likely that in humans they determine parasite virulence.
135
136 **Results**
137
138 **GRA15 and GRA24 regulate murine macrophage function *in vitro***

Synthesis of IL12 by *Toxoplasma*-infected macrophages was previously shown to be dependent on p38 MAPK and NFκB activation (44, 45). Indeed, deletion of either *GRA15* or *GRA24* significantly reduced macrophage IL12/IL23p40 production, consistent with their activation of the NFκB and p38 MAPK pathway, respectively (31, 35). It was previously shown that GRA24 from both type I RH and type II Pru strains activates the p38 MAPK pathway. However, the GRA24-dependent transcriptional changes in murine macrophages are much more pronounced after infection with type II strains compared to type I strains (35). For example, without GRA24 the Pru induction of inflammatory cytokines, including IL12/IL23p40, is significantly affected, while GRA24 only has a minor effect on the modulation of these cytokines by RH. It is possible that many of the GRA24-mediated transcriptional changes are dependent on GRA15, as RH does not express a functional GRA15 (31). To more directly test whether GRA15 and GRA24 have any synergistic or additive effect on macrophages, we generated *gra24* single knockout and *gra15*/*gra24* double knockout parasites in the type II Pru strain (**Suppl. Fig. 1**). We infected murine bone marrow derived macrophages (BMDMs) with Pru wild-type, Δ*gra15* (31), Δ*gra24* and Δ*gra15/24* parasites for 24 h and measured the release of IL12/IL23p40, IL1β and TNFα, which are cytokines often used as M1 macrophage polarization markers (38). BMDMs infected with Δ*gra15* or Δ*gra15/24* parasites secreted significantly less IL12/IL23p40, IL1β and TNFα (**Fig. 1a-c**) compared to wild-type infected BMDMs. Deletion of *GRA24* significantly impaired the release of IL12/IL23p40 but had no effect on IL1β and TNFα (**Fig. 1a-c**). We also measured arginase activity (a marker for M2 macrophages) in macrophages infected with Δ*gra15*, Δ*gra24* or Δ*gra15*/*24* parasites. Δ*gra24* and Δ*gra15/24*, but not wild-type and Δ*gra15*

parasites, induced significant arginase activity in macrophages (**Fig. 1d**). The transcription of the p40 subunit of IL12 in mice is primarily dependent on cREL and moderately on the NFκB p65 subunit (46). Macrophages infected with wild-type parasites contained significantly more nuclear (activated) cREL compared to macrophages infected with Δ*gra15*, Δ*gra24* or Δ*gra15/24* parasites (**Fig. 1e**). Similar results were obtained in human foreskin fibroblasts (HFFs) (**Suppl. Fig. 3**). Nuclear translocation of the NFκB p65 subunit in macrophages and HFFs was significantly reduced after infection with Δ*gra15* or Δ*gra15*/*24* parasites but not after infection with Δ*gra24* parasites (**Suppl. Fig 1e and f**). Thus, our results show that while GRA15 is required for the secretion of IL1β and TNFα from BMDM, both GRA15 and GRA24 are required for the secretion of IL12/IL23p40.

## Deletion of *GRA15* and *GRA24* affects *in vivo* parasite growth and cytokine production in *Tlr11*$^{-/-}$ mice

It was previously shown that the intraperitoneal parasite load in C57BL/6 mice intraperitoneally (i.p.) infected with either Δ*gra15* or Δ*gra24* was higher compared to wild-type parasites, but the mortality of the mice was not significantly different (31, 35). To determine if *Toxoplasma* profilin-mediated activation of TLR11 might have masked the effect of GRA15 and GRA24 we investigated parasite burden and mortality in the *Tlr11*$^{-/-}$ mice. *Tlr11*$^{-/-}$ mice i.p. infected with Δ*gra15, Δgra24* or Δ*gra15/24* parasites had a significantly larger peritoneal parasite load 3 days p.i. compared to wild-type infected mice, with Δ*gra15*-infected mice having the highest parasite load (**Fig. 2a**). On day 1 p.i., the level of IL12/IL23p40, IFNγ, IL1β or TNFα in the serum was not higher than in uninfected mice (not shown). It was recently shown that in *Tlr11*$^{-/-}$ mice IL18 is

necessary and sufficient for induction of IFNγ production (43). The IL18 level was significantly increased in mice infected with wild-type parasites (**Fig. 2b**) while mice infected with Δ*gra15* or Δ*gra24* parasites had significantly lower serum IL18 levels on day 1 p.i. compared to wild-type parasite infected mice, which was even further reduced in mice infected with Δ*gra15/24* parasites. On day 1 p.i. IFNγ, IL18, IL1β or TNFα were not detected in the peritoneal fluid (not shown) but the IL12/IL23p40 levels were significantly higher in mice infected with wild-type parasite compared to uninfected mice (**Suppl. Fig. 4a**). Mice infected with Δ*gra15/24* parasites contained significantly lower IL12/IL23p40 levels compared to wild-type parasite infected mice (**Suppl. Fig. 4a**). On day 3 p.i., the IL18 level in serum still remained significantly higher in wild-type parasite infected mice, while Δ*gra15,* Δ*gra24* or Δ*gra15/24* parasites elicited significantly lower IL18 levels (**Fig. 2c**). Although IL12/IL23p40 levels were significantly lower at day 3 p.i. in sera of mice infected with Δ*gra15/24* parasites compared to wild-type infected mice (**Fig. 2d**), this difference was not detected in the peritoneal fluid (**Fig. 2f**). On day 3 p.i., there was a large increase in IFNγ in both serum and peritoneal fluid of wild-type parasite infected mice (**Fig. 2e and g**) which was significantly decreased in mice infected with Δ*gra15* and Δ*gra24* parasites, and even further decreased in mice infected with Δ*gra15/24* parasites (**Fig. 2e and g)**. All *Tlr11*$^{-/-}$ mice i.p. infected with wild-type or Δ*gra15/24* parasites died by day 10 p.i. with similar severe reduction in body weight (**Suppl. Fig. 4b and c**). Thus, GRA15 and GRA24 both contribute to induction of IFNγ from *Tlr11*$^{-/-}$ mice by inducing IL18 and IL12, which impacts the early intraperitoneal parasite load.

It was previously described that *Tlr11*$^{-/-}$ mice can survive i.p. infection with tissue cysts (20-25 cysts) (5, 6, 42). In our hands, however, all *Tlr11*$^{-/-}$ mice i.p. infected with 10 cysts of wild-type or Δ*gra15/24* parasites succumbed by day 13 p.i. with similar body weight reduction, although the Δ*gra15/24* parasites caused significantly earlier mortality (**Suppl. Fig. 4d and e**). Because of the unexpected extreme susceptibility of the *Tlr11*$^{-/-}$ mice after i.p infection with tachyzoites or with tissue cysts, we performed s.c. infections to curb rapid *Toxoplasma* dissemination. Compared to wild-type, Δ*gra15/24* parasites caused significantly more mortality in s.c. infected *Tlr11*$^{-/-}$ mice (**Fig. 2h**), whereas Δ*gra15* and Δ*gra15/24* parasites caused a significantly larger body weight reduction (**Fig. 2i**). Thus, GRA15 and GRA24 have a significant effect on the innate immune response in *Tlr11*$^{-/-}$ mice. However, these mice are already extremely susceptible to wild-type parasite infection and an increased virulence of parasites without GRA15 and/or GRA24 can therefore not be detected after i.p. infection.

## The *ROP18* and *ROP5* allelic combinations determines survival of *Tlr11*$^{-/-}$ mice

Although there was a significant difference in cytokine induction in *Tlr11*$^{-/-}$ mice i.p. infected with Δ*gra15,* Δ*gra24* or Δ*gra15/24* parasites (**Fig. 2b-g**), all mice succumbed within 10-13 days p.i. In mice, acute parasite virulence is determined by the exact *ROP18* and *ROP5* allele (10, 47–50). To determine the role of ROP18 and ROP5 in *Tlr11*$^{-/-}$ mice we i.p. infected *Tlr11*$^{-/-}$ mice with 4 F1 progeny (S22, S26, STE10 and CL13) from a type IIxIII cross (51) that have the avirulent alleles of *ROP18* and *ROP5*. While 100% mortality was observed after infection with 100 Pru wild-type or Δ*gra15/24* parasites (**Suppl. Fig. 4b**), mice infected with these F1 progeny strains survived doses up to $10^5$ parasites (**Fig. 2h and i**). Only 1 mouse infected with CL13 and 2 mice

infected with STE10 parasites (out of 5) died at the $10^7$ dose (**Fig. 2j**), accompanied with significant body weight reduction (7-10%) only in mice infected with the STE10 strain (**Suppl. Fig. 4f-h**). Thus, although in *Tlr11*$^{-/-}$ mice the cytokine response is significantly influenced by GRA15 and GRA24, survival after i.p. infection is almost entirely dependent on ROP18 and ROP5. It therefore appears that *Tlr11*$^{-/-}$ mice are not a good model for the human immune response to *Toxoplasma* as humans do not have IRGs and ROP18 and ROP5 do not affect *Toxoplasma* resistance to IFNγ in human cells (10, 17, 52).

## GRA15 and GRA24 induce cytokine secretion in human macrophages through activation of p38 MAPK and NFκB

The innate immune response against *Toxoplasma* in human monocytes is affected by the infecting strain type. For example, type II, but not type I strains, are major inducers of IL1β (18, 33), which is primarily dependent on type II GRA15 (33). However, the role of GRA24 in the induction of pro-inflammatory cytokines by human macrophages is not known. We measured IL12/IL23p40, IL1β and TNFα from THP1-derived macrophages infected with wild-type, Δ*gra15*, Δ*gra24* and Δ*gra15/24* parasites and observed that, akin to murine macrophages, GRA15 and GRA24 were both important for generation of IL12/IL23p40 (**Fig. 3a**). However, in contrast to murine macrophages, both GRA15 and GRA24 determined IL1β and TNFα production by THP1-derived macrophages (**Fig. 3b-c**). This difference between human and murine macrophages could be due to species-specific transcription factor dependence as often seen specifically for macrophages (53). We also measured the growth of the different parasite lines in THP1 macrophages and detected a growth advantage in parasites lacking *GRA24* compared to wild-type

parasites (**Fig. 3d**). Furthermore, similar to murine macrophages, while GRA15 and GRA24 specifically activated nuclear translocation of p65 NFκB and p38 MAPK, respectively, in THP1 macrophages (**Fig. 3e and f, Suppl. Fig. 5a-b**), both GRA15 and GRA24 were required for nuclear translocation of cREL (**Fig. 3g and Suppl. Fig. 5c**). To confirm the role of NFκB and p38 MAPK on cytokine secretion from THP1 macrophages, we inhibited the two pathways using BAY11-7082, an irreversible inhibitor of IκB phosphorylation important for NFκB activation (54) and BIRB796, a potent inhibitor of p38 MAPKα (55), respectively. Inhibition of either the NFκB or p38 MAPK pathway significantly inhibited the secretion of IL12/IL23p40 and IL1β from THP1 macrophages infected with wild-type parasites (**Fig. 3h and i**), while the inhibitors did not affect parasite growth (**Fig. 3j**). Thus, GRA15 and GRA24 regulate pro-inflammatory cytokine production from THP1-derived macrophages through NFκB- and p38 MAPK-dependent pathways.

## IL12 and NLRP3 inflammasome-derived IL18 induce the secretion of IFNγ from human PBMCs

In mice, IFNγ is known to be induced by IL12, which can be further enhanced by IL18 and IL1β (14, 15). To determine the role of IL12 and IL18 in the induction of IFNγ in human cells we used PBMCs as a model (56). When PBMCs were infected with Pru wild-type there was a significant decrease in IFNγ secretion upon blocking IL12 or IL18 compared to either untreated or isotype antibody-treated cells (**Fig. 4a**), which was more pronounced when cells were treated with blocking antibodies against both IL12 and IL18. These results suggest that both IL12 and IL18 are required for optimal IFNγ production by human PBMC (**Fig. 4a**). This was further corroborated by the increased

parasite growth detected in PBMCs treated with blocking antibodies against IL12, IL18, or both (**Fig. 4b**). IL18 and IL1β are secreted as a result of inflammasome activation (12). In *Toxoplasma*-infected human PBMCs, IL1β secretion is mediated via NLRP3 inflammasome activation (20). Indeed, inhibition of the NLRP3 inflammasome with MCC950 or inhibition of CASP1 with VX765 led to a significant decrease in IL1β, IL18, and IFNγ secretion (**Fig. 4c-e**) accompanied by increased parasite growth (**Fig. 4g**). These effects on IFNγ by the inhibitors were not dependent on IL12/IL23p40 secretion, as the inhibitors did not alter IL12/IL23p40 levels (**Fig. 4f**). Thus, IFNγ secretion from human PBMCs infected with the type II Pru strain, is dependent on IL12 and NLRP3 inflammasome-derived IL18 and IL1β.

**Cytokine secretion from human PBMCs is mediated through activation of NFκB and p38 MAPK by GRA15 and GRA24**

To test whether p38 MAPK and NFκB signaling are involved in cytokine production from PBMCs infected with Pru wild-type, we used the inhibitors BIRB796 (inhibits p38 MAPK) and BAY11-7082 (inhibits IκB phosphorylation). Both inhibitors inhibited secretion of IL12/IL23p40 (**Fig. 5a**), IL1β (**Fig. 5b**) and IFNγ (**Fig. 5c**), with BAY11-7082 having a much greater effect (**Fig. 5a-c**). Furthermore, compared to untreated PBMCs, those treated with either of these inhibitors supported more parasite growth (**Fig. 5d**). As we observed that GRA15 and GRA24 induced inflammatory cytokine generation in THP1-derived macrophages, we also tested their effect on human PBMCs. PBMCs infected with Δ*gra15*, Δ*gra24*, or Δ*gra15/gra24* parasites secreted significantly less IL12/IL23p40 compared to PBMCs infected with wild-type parasites (**Fig. 6a**). Furthermore, parasites lacking *GRA15*, *GRA24*, or both grew more in PBMCs compared to wild type parasites

probably due to lack of anti-parasitic IFNγ secretion from PBMCs infected with the knockout parasites (**Suppl. Fig. 6a**). Likewise, PBMCs infected with Δ*gra15*, Δ*gra24*, or Δ*gra15/gra24* parasites secreted significantly less IFNγ, TNFα and IL1β compared to PBMCs infected with wild-type (**Fig. 6b-d**). Thus, GRA15 and GRA24 together determine the secretion of proinflammatory cytokines IL12/23p40, IFNγ, TNFα and IL1β from infected human PBMCs.

Recently, it was shown that in humans, alarmin S100A11 is released from *Toxoplasma*-infected fibroblasts and sensed by THP1 monocytes, which upregulated CCL2 production to induce recruitment of additional monocytes (18). However, the secretion of alarmin S100A11 did not differ between uninfected and parasite infected PBMCs (**Suppl. Fig. 6b**). Nevertheless, akin to a previous study (18), HFFs infected with wild-type parasites secreted significantly more S100A11 compared to uninfected cells, which could be due to increased activity of inflammatory caspases 1 and 4 (**Suppl. Fig. 6c-d**). Secretion of S100A11 is dependent on permeabilization mediated cell lysis (18) and fibroblasts treated with Triton X100 released very high level of S100A11 (**Suppl. Fig. 6b**). HFFs infected with type II strains underwent significant cell death possibly explaining the increase in S100A11 release (data not shown). Our data indicate that inflammatory cytokine secretion from human PBMCs infected with type II *Toxoplasma* is regulated by both GRA15 and GRA24.

## Discussion

Innate recognition of *Toxoplasma gondii* DNA/RNA and profilin by nucleic acid sensing TLRs or TLR11/12 heterodimers is critical for robust IL12 production and subsequent activation of host protective IFNγ (7, 57, 58). Nevertheless, hosts lacking TLR11/12 can

still produce IL12 from monocytes and dendritic cells while IFNγ is produced from T cells, NK cells and neutrophils (18, 42, 43, 56). Our study showed that, compared to wild-type parasite infected mice, *Tlr11*$^{-/-}$ mice infected with parasites lacking *GRA15* and/or *GRA24* have an increased parasite load which was correlated with significantly lower IL18, IL12 and IFNγ levels. However, even in the *Tlr11*$^{-/-}$ mouse model, parasite virulence is primarily determined by ROP18 and ROP5. ROP18 and ROP5 counteract the IRGs, which are not present in humans, and which likely explains why ROP18 and ROP5 do not determine parasite susceptibility to human IFNγ (10, 17, 52). Thus *Tlr11*$^{-/-}$ mice do not appear to be a good model for the human immune response to *Toxoplasma*. We show that in human THP1 derived macrophages GRA15 and GRA24 induced IL12, TNFα and IL1β through their ability to activate the NFκB and p38 MAPK pathways. In PBMCs we show that IFNγ secretion is dependent on IL12 and NLRP3 inflammasome-derived IL18 and IL1β, which are also induced by GRA15 and GRA24. Thus, GRA15 and GRA24 are major activators of the human immune response.

In the murine model of toxoplasmosis, IL12 production is largely dependent on dendritic cells (DCs) and macrophages (4, 44, 59, 60). However, the mechanism of IL12 production by these two cell types is different (8), as in DCs it is primarily determined by TLR11, chemokine receptor 5 (CCR5) and the myeloid differentiation factor 88 (MyD88) pathway, with an additional role of G protein coupled receptor signaling (GPCR) (4, 61, 62). On the other hand, generation of IL12 from macrophages is independent of TLR11 and is induced primarily by cREL NFκB driven transcription (8, 63). Additionally, compared to cREL NFκB, p65 NFκB plays a moderate role in induction of IL12/1L23p40 (46). The larger impact on IL12/IL23p40 production by GRA15 compared to GRA24

might be due to the activation of both p65 and cREL by GRA15, while GRA24 only activates cREL. TNFα and IL1β are regulated by the NFκB p65-p50 subunit in murine macrophages (46) which explains why these cytokines were not affected by GRA24.

Compared to an *in vitro* cell culture system, the immune response *in vivo* is much more complex, as multiple cell types interact and can exert a considerable influence on disease outcome. For instance, although *Tlr11*$^{-/-}$ mice lack the increased level of IL12 compared to wild-type mice upon *Toxoplasma* infection (4, 5, 57) the IFNγ response in these mice is intact and even higher than in wild-type mice, possibly due to the higher parasite load (42, 43, 57). One important gap in these studies is the determination of what parasitic factors are responsible for the residual IL12 or IL18 that activate NK and T cells to produce IFNγ. Although, GRA15 and GRA24 control cytokine induction in *Tlr11*$^{-/-}$ mice, a significant level of IFNγ was still detected in *Tlr11*$^{-/-}$ mice infected with Δ*gra15/24* parasites. This is probably due to the release of parasite derived nucleic acids after IRG and GBP-mediated destruction of the PVM, which can induce interferon production through nucleic acid sensing TLRs (57, 64). Mice lacking either *Tlr11*$^{-/-}$ or *Tlr3/7/9*$^{-/-}$ still produce IL12 and IFNγ upon *Toxoplasma* infection, whereas in 3d mice (lacking the endosomal chaperone UNC93B1 for all TLR 3/7/9/11/12) or *Tlr3/7/9/11*$^{-/-}$ quadruple knockout mice, the IL12 and IFNγ response was completely abrogated (57). This could explain why a significant level of IFNγ in *Tlr11*$^{-/-}$ mice infected with Δ*gra15/24* parasites was still detected.

It was previously shown that *Tlr11*$^{-/-}$mice infected with ME49 tissue cysts were not more susceptible compared to wild-type mice (42, 57). By contrast, in our study acute susceptibility of *Tlr11*$^{-/-}$ mice was observed when infected with either a low number of

Pru cysts or tachyzoites which was accompanied by a steady reduction of body weights. Similarly, a recent study showed an increased susceptibility of *Tlr11*$^{-/-}$ mice after ME49 infection (43). This variable susceptibility of *Tlr11*$^{-/-}$ mice could be due to the parasite strains used for infection, i.e ME49 *versus* Pru, which can elicit a different immune response (65). Alternatively, the different susceptibility of *Tlr11*$^{-/-}$ mice could be explained by variations in the microbiota in these mice, as they were housed in different colonies (5, 42, 43, 57, 66)(43). Acute mortality of mice upon *Toxoplasma* infection depends on the route of infection and virulence of the parasite strain (67). For virulent parasites a difference between knockout and wild-type parasites is more likely to be detected after s.c. infections, as this results in a slower dissemination of parasites from the site of infection (32). Similarly, in our study significantly enhanced virulence of Δ*gra15/24* parasites compared to Pru wild type was only observed after s.c. infection.

The human immune response to *Toxoplasma* has been studied in THP1 monocytes (18, 33), isolated PBMCs (18), or elutriated monocytes (18, 20, 56). Previous studies have shown that although THP1 monocytes infected with type II strains secrete IL1β (18, 33), they do not secrete IL12/IL23p40 (18). However, we observed that PMA-differentiated THP1 macrophages secreted both IL12/IL23p40 and IL1β in a GRA15- and GRA24-dependent way. This could be attributed to differences between monocytes used in those studies (18, 33) versus macrophages in our study as primary human monocytes and macrophages from the same donor differ in their cytokine secretion pattern (20, 56). In the present work, we detected a large amount of IL12/IL23p40 secretion from *Toxoplasma* infected PBMCs. This is in accordance with Tosh *et al. (56)*, where they showed that elutriated monocytes or column purified monocytes were

391 equally efficient in secreting IL12/IL23p40 secretion upon *Toxoplasma* infection
392 regardless of the strain type. On the other hand, Safronova et al. (18) did not observe
393 any IL12/IL23p40 secretion from PBMCs infected with type II *Toxoplasma*. This
394 discrepancy could be due to differences in the isolation and purification of monocytes,
395 time point of the assay and, most importantly, the multiplicity of infection (MOI) (68).

396 THP1 cells are a homogenous monocytic cell population, whereas human PBMCs
397 contain a mixture of cell types comprising a small proportion (approx. 10%) of
398 monocytes (69). T cells constitute the largest fraction of PBMCs (roughly ¾ th), and
399 IFNγ production by these cells is primarily determined by IL12 and IL18-mediated
400 activation of STAT4, p38 MAPK, NFκB, and activator protein 1 (AP-1) family of
401 transcription factors, respectively (70). It has been shown that within human PBMCs
402 *Toxoplasma* preferentially infects monocytes but lymphocytes were also infected at a
403 lower level (71, 72). Based on these facts and the results observed in our study, we
404 hypothesize that in human PBMCs the parasite-infected monocytes produce IL12
405 through cREL activation and IL18 by inflammasome activation (73), which together
406 activate T cells to produce anti-parasitic IFNγ which could destroy some PVs.
407 Subsequently, PAMPs get released inside the host cytosol and could be sensed by
408 cytosolic nucleic acid sensing TLRs such as TLR3/7/9, in turn inducing IL12. Indeed, it
409 has been shown that IFNγ-primed human PBMCs produce IL12, IL1β and TNFα when
410 treated with type II parasite derived DNA and RNA (57). Taken together, we determined
411 that the immune response against *Toxoplasma* in TLR11 deficient mice or human cells
412 is largely dependent on GRA15/GRA24-induced inflammasome-mediated secretion of
413 IL18/IL-1β which together with IL12 activate NK and T cells to secrete IFNγ that kills the

parasite. Our study advances our understanding of the human immune response against *Toxoplasma*.

## Materials and Methods

### Culture of cells and parasites

Human foreskin fibroblasts (HFFs) and RAW 264.7 macrophages were cultured as described previously (31, 74). All parasite lines were maintained *in vitro* by serial passage on HFFs monolayers and cultured in the same medium as HFFs but with 1% fetal bovine serum FBS). A *Toxoplasma gondii* Pru strain expressing firefly luciferase and GFP (PruΔ*hpt*, PruA7) was used as representative of type II (75).

### Generation of bone marrow-derived macrophages and THP1 macrophages

Bone marrow-derived macrophages (BMDMs) were isolated from C57BL/6 mice and cultured as described previously (13). THP1 monocytes were cultured in RPMI-1640 supplemented with 10% FBS, 2 mM L-glutamine, 100 U/mL penicillin/streptomycin and 10 mg/mL gentamicin. For differentiation into macrophages, THP1 monocytes were stimulated with 100 nM phorbol 12-myristate 13-acetate (PMA) for 3 days and then rested for 1 day with replacement of the PMA containing medium with complete medium without PMA before performing experiments. All the experiments involving THP1 monocytes were performed with passage numbers <10.

### Generation of knockout parasites

It was previously shown that type II *Toxoplasma* strains lacking hypoxanthine-guanine phosphoribosyltransferase (*HXGPRT* or *HPT*) are more virulent than strains having *HPT* (76). To remove the *HPT* gene from the Δ*gra15* strain, we mutated the *HPT* locus (TGME49_200320) by using a clustered regularly interspaced short palindromic repeat (CRISPR)-Cas9 based system. The sgRNA sequence against *HPT* (**Table 1**) was cloned into the pSS013-Cas9 vector (pU6 plasmid, Addgene plasmid # 52694) using the *BsaI* specific sites. To generate PruΔ*gra15*Δ*hpt*, the circular pSS013-Cas9 vector containing the sgRNA against *HPT* was transfected (10 µg) as described elsewhere (77). For the selection of Δ*hpt* parasites, single clones were grown in parallel with Mycophenolic acid (MPA)-Xanthine (25 µg/mL) and 6-Thioxanthine (177 µg/mL) containing media. Parasites that were able to grow in 6-Thioxanthine but not in MPA-xanthine media were selected and further confirmed by PCR and sequencing (**Table 1**). To disrupt *GRA24* (TgME49_230180) in PruΔ*hpt* and PruΔ*hpt*Δ*gra15* strains, the pSS013-Cas9 vector containing a sgRNA against *GRA24* was transfected along with *NotI* (New England Biolabs) linearized pLoxP-DHFR-mCherry-LoxP (Addgene Plasmid #70147), at a 5:1 molar ratio, as described previously (77). This plasmid contains a pyrimethamine resistance cassette tagged with the fluorescence marker mCherry and flanked by two LoxP sites. After three rounds of pyrimethamine selection (1 µM) and limiting dilution cloning, *GRA24* knockout parasites were assessed by PCR and confirmed by sequencing (**Table 1**). To flox out DHFR-mCherry, Δ*gra24* and Δ*gra15/24* parasites were transfected with a plasmid (78) expressing Cre recombinase (50 µg) as described above. Single clones were checked for their inability to grow in the presence of pyrimethamine and absence of mCherry.

## Generation and maintenance of *Tlr11*$^{-/-}$ mice

To generate the *Tlr11*$^{-/-}$ mouse colony, two 4-week-old *Tlr11*$^{-/-}$ male mice (42, 66) were bred with wild-type female C57BL/6 mice (Jackson laboratories). The *Tlr11*$^{+/-}$ F1 progeny mice were subsequently crossed to obtain *Tlr11*$^{-/-}$ mice. Genotyping of F2 individuals was performed by PCR from DNA isolated from tail clips to identify the hybrid or homozygous variants (**Table 2**, **Suppl. Fig. 2**). Once the homozygous mice were confirmed by PCR genotyping (**Suppl. Fig. 2**), they were bred to get the entire colony of *Tlr11*$^{-/-}$ mice. Mice were maintained at the University of California, Davis (UC Davis) mouse housing facility, where water and feed were provided *ad libitum*. Animal experiments were performed in strict accordance with the recommendations in the Guide for the Care and Use of Laboratory Animals of the National Institutes of Health and the Animal Welfare Act, approved by the Institutional Animal Care and Use Committee at UC Davis (assurance number A-3433-01).

## *In vivo* infection, parasite burden and cytokine measurement

Male and female 6–10-week-old *Tlr11*$^{-/-}$ mice were used in the experiments. For infection, tachyzoites were cultured in HFFs and extracted from host cells by passage through 27- and 30-gauge needles, washed two times in PBS, and quantified with a hemocytometer. Parasites were diluted in PBS, and mice were inoculated either i.p. or s.c. with tachyzoites of each strain (100-5,000 tachyzoites in 200 µl) using a 29-gauge needle. Body weights were recorded every day and for survival analysis mice were kept for 30 days. To obtain brain cysts, 5,000 tachyzoites of wild-type and Δ*gra15/24* parasites were injected i.p. into CD1 mice (Charles River) and 4 weeks later these mice were sacrificed, brains aseptically collected and cysts isolated for both strains (41).

Subsequently, 10 cysts of each parasite strain were infected i.p. into *Tlr11*$^{-/-}$ mice to determine survival and body weight reduction.

*In vivo* parasite burden was measured by i.p. infecting 5,000 tachyzoites into *Tlr11*$^{-/-}$ mice for 3 days. Subsequently, peritoneal fluids were collected and cells isolated by centrifugation. A total of $1\times10^5$ cells were plated in 96-well plates in triplicate for each group for 24 h. Following incubation, supernatants were removed and lysis buffer was added prior to measure relative parasite growth by luciferase assay (74).

To quantify cytokines *in vivo*, mice were sacrificed on day 1 or 3 p.i. to collect blood and peritoneal fluid. Serum was diluted 1:10 for IL12/IL23p40 and 1:20 for IFNγ and TNFα measurement. IFNγ, IL12/IL23p40, and TNFα levels were determined using commercially available matched pair ELISA kits (Invitrogen, Thermo Fisher Scientific), following the manufacturer's instructions.

### ***In vitro*** **parasite growth determination**

Freshly confluent HFFs 24-well plates were used to determine relative parasite growth by plaque assay. On the day of infection, the media was replaced and 250 freshly harvested parasites were added to each well. Plates were then left undisturbed for 6 days at 37 °C 5% $CO_2$, after which plaque areas were imaged and measured. Plaque areas were captured and analyzed using a Nikon TE2000 inverted microscope equipped with Hamamatsu ORCA-ER digital camera and NIS Elements Imaging Software, respectively. For all experiments, at least 20-25 plaques from technical duplicate wells were imaged. For measurement of total parasite growth, a luciferase-based assay was performed (74).

## Immunofluorescence detection of p65 (NFκB), p-p38 MAPK and c-REL (NFκB) nuclear translocation

Immunofluorescence to detect nuclear translocation of p65 (NFκB), p-p38 MAPK and c-REL was done in HFFs, MEFs, RAW 264.7 macrophages and THP1-derived macrophages using the following antibodies: rabbit anti p65 (1:200 dilution, sc-109, Santacruz Biotechnology, CA, USA), rabbit anti p-p38 MAPK (1:800 dilution, #4511, Cell Signaling Technology, MA, USA), rabbit anti cREL (1:500 dilution, #4727, Cell Signaling Technology, MA, USA) and mouse anti cREL (1:200 dilution, NBP2-37593, Novus Biologicals, CO, USA for RAW 264.7 macrophages). Briefly, cells were plated on coverslips in 24-well plates ($1\times10^5$ cells/well) and subsequently infected with *Toxoplasma* with a MOI of 3 for 24 h. Following incubation, cells were fixed with 3% formaldehyde, permeabilized and blocked with buffer containing 0.2% Triton X-100 along with 3% BSA and 5% goat serum. Cells were incubated with primary antibodies overnight at 4 $^{\circ}$C, after which each well was washed 3 times with 1×PBS, followed by incubation with goat anti rabbit Alexa fluor 594 (1:1,000 dilution, Invitrogen) and Hoechst 33258 (1:500 dilution, Invitrogen, Thermo Fisher Scientific) for 1 h. Finally, coverslips were washed 5 times with 1×PBS and mounted with VECTASHIELD antifade mounting medium (Vector Laboratories, CA, USA). Nuclear intensity of at least 15 infected cells was measured for each experiment and coverslip.

## Isolation of human peripheral blood mononuclear cells (PBMCs)

PBMCs were isolated from leukocyte reduction chambers (LRS) from individual donors, which were purchased from BloodSource (CA, USA) and tested seronegative for *Toxoplasma*. After collecting the blood from the LRS according to the manufacturer's

525 protocol using sterile needles and blades, PBMCs were isolated using ficoll-Paque
526 premium 1.077 gm/dL (GE Healthcare, PA, USA) as described previously (79). Isolated
527 PBMCs were subsequently used for experiments using RPMI-1640 supplemented with
528 10% FBS, 2 mM L-glutamine, 100 U/mL penicillin/streptomycin and 10 mg/mL
529 gentamicin or kept frozen in 90% FBS and 10% dimethyl sulfoxide (DMSO) for later
530 use.

531 ***In vitro* cytokine ELISA**

532 C57BL/6 BMDMs, Raw 264.7 macrophages, THP1 macrophages or PBMCs were
533 seeded ($1\times10^5$ cells per well) in 96-well plates at 37 °C in 5% $CO_2$. Cells were infected
534 with freshly lysed tachyzoites of the different parasite strains at MOI = 3, 5 and 7, and
535 supernatants (200 µl) were collected 24 h p.i. and used to determine IL12/IL23p40,
536 IL1β, TNFα, IL18 and IFNγ levels. To verify that cells were infected with equal numbers
537 of viable parasites, plaque assays were performed as described above. Cytokine levels
538 were measured using a commercially available matched pair ELISA kit (Invitrogen,
539 Thermo Fisher Scientific) following the manufacturer's instructions.

540 In some assays, THP1 cells or PBMCs were first treated 2 h prior to infection with
541 different inhibitors: BAY 11-7082 at 5 µM, (APExBIO, TX, USA), BIRB796 at 10 µM
542 (Tocris Bioscience, MN, USA), VX765 at 50 µM (Sellelckchem, TX, USA) and MCC950
543 at 10 µM (Adipogen Life Sciences, CA, USA), and culture supernatants collected after
544 20 h. A total of 30 µL of cell lysis buffer was added per well and a luciferase-based
545 growth assay was performed as mentioned above.

For IFNγ determination in IL12 and/or IL18 neutralized conditions, PBMCs were first infected with Pru wild-type parasites and 1 h p.i. cells were treated with either 2 µg/mL of IL12, IL18 or isotype specific antibodies (MBL International, Japan), or both IL12 and IL18 together for another 20 h before harvesting the culture supernatant. Parasite growth was measured by luciferase assay as described above.

**Measurement of alarmin S100A11 by ELISA**

Alarmin S100A11 was measured by using a commercially available pre-coated kit from RayBiotech (GA, USA). Briefly, PBMCs ($1\times10^5$ cells/well) or HFFs ($2\times10^4$ cells/well) were seeded in 96-well plates at 37 °C in 5% $CO_2$ and subsequently infected with freshly lysed tachyzoites of the different parasite strains at MOI = 3, 5 and 7, and supernatants (100 µl) were collected 24 h p.i. As a positive control for S100A11 secretion, 2% Triton X-100 was used in complete medium. To compare the level of S100A11 secretion between different strains, parallel plaque assays were performed.

**Arginase assay from macrophages**

Arginase activity was measured from lysates of RAW 264.7 macrophages infected with different strains of *Toxoplasma* 24 h p.i in a 96-well plate with three different MOIs each time as described previously (74). To determine that cells were infected with equal numbers of viable parasites, plaque assays were performed as described above and values relativized.

**Caspase 1/4/5 activity assay**

Activity of the inflammatory caspases 1/4/5 was measured using a commercially available Caspase-Glo® 1 Inflammasome Assay (Promega, WI, USA) from HFFs

568 seeded in 96-well plates ($2\times10^4$ cells per well). HFFs were pre-treated with an inhibitor
569 of caspases 1/4/5 (VX765 at 50 µM) 2 h before infection and subsequently infected with
570 Pru wild-type parasites for another 20 h. Caspase activity was measured from the lysate
571 and data were recorded from a single channel luminometer with a 10 s delay program.

572

573

574

575

576 **Figure Legends**

577 **Figure 1: GRA15 and GRA24 activate the *in vitro* macrophage response**

578 BMDMs were infected with indicated *Toxoplasma* strains for 24 h and IL12/IL23p40 (**a**),
579 IL1β (**b**) and TNFα (**c**) were measured in the supernatant. Experiments were done 3
580 times. Arginase activity was measured (**d**) from RAW 264.7 macrophages infected with
581 indicated strains 24 h p.i. Nuclear translocation of the cREL subunit of NFκB (**e**) was
582 quantified from infected RAW 264.7 macrophages 18 h p.i. with indicated strains. In
583 each experiment at least 15 cells were quantified as shown in the graph (left) and
584 experiment was done 3 times (right panel graph). A representative image for each
585 group is shown in the middle panel. Scale bar is 10 µm. Each dot represents the mean
586 of 3 technical replicates from individual experiments, except for the scatter diagram in
587 (e). Statistical analysis was done by two sample student's t test for figures a-e. Data are
588 represented as mean ± standard error of the mean (SEM).

589 **Figure 2: Deletion of *GRA15* and *GRA24* leads to enhanced parasite virulence in**
590 ***Tlr11*$^{-/-}$ mice**

591 *Tlr11*$^{-/-}$ mice were i.p. infected with 5,000 tachyzoites of indicated *Toxoplasma* strains
592 expressing luciferase, and serum and peritoneal fluid were collected from each mouse
593 (N=3 mice per group) at different time points. (**a**) Three days p.i. peritoneal cells were
594 isolated, plated in tissue culture plates for 24 h and the following day luciferase reading
595 was taken to measure the parasite burden. (**b**) Serum IL18 levels at 1 day p.i. Serum

596 IL18 (**c**), IL12/IL23p40 (**d**) and IFNγ (**e**) levels 3 days p.i. IL12/IL23p40 (**f**) and IFNγ (**g**)
597 levels in the peritoneal fluid 3 days p.i. All data represent mean ± SEM. Statistical
598 analysis was done with two sample Student's t tests. *Tlr11*$^{-/-}$ mice were s.c. infected with
599 5,000 tachyzoites of indicated strains and (**h**) survival and (**i**) weight (plotted as an
600 average of the change in body weight for each cohort, where 100% body weight
601 corresponds to the day of infection) of the mice were monitored for 30 days. Statistical
602 analysis was done using a log-rank test. N=8 each for wild-type and Δ*gra15/24* whereas
603 N=5 for Δ*gra15* and Δ*gra24. Tlr11*$^{-/-}$ mice were i.p injected with indicated doses of
604 tachyzoites of different *Toxoplasma* strains derived from F1 progenies of a type II X type
605 III cross (51) containing avirulent *ROP18* and *ROP5* alleles and survival was monitored
606 (**j**). Each dot represents a mean of 3 technical replicates from an experiment. Statistical
607 analysis was done by two sample student's t test for figures a-g. Data are represented
608 as mean ± standard error of the mean (SEM).

609 **Figure 3: GRA15 and GRA24 activate pro-inflammatory cytokine secretion by**
610 **human macrophages.**

611 THP1 monocyte-derived macrophages were infected with indicated *Toxoplasma* strains
612 for 24 h, after which IL12/IL23p40 (**a**), IL1β (**b**) and TNFα were measured. Relative
613 parasite growth was measured by luciferase growth assay (**d**). Nuclear translocation of
614 the NFκB p65 (**e**), p-p38 MAPK (**f**), and NFκB cREL (**g**) subunits were quantified from
615 infected THP1 macrophages 18 h p.i with indicated strains. In each experiment at least
616 15 cells were quantified. THP1 macrophages were treated with indicated inhibitors 2 h
617 prior to infection and subsequently infected for an additional 20 h. IL12/IL23p40 (**h**),
618 IL1β (**i**) and growth (**j**) were measured. Each dot represents a technical mean value

from a single experiment, and each experiment was done 3 times. Statistical analysis was done by One way ANOVA followed with Tukey's multiple comparison test. Data are represented as mean ± standard error of the mean (SEM).

**Figure 4: Secretion of IFNγ from human PBMCs is dependent on IL12 and NLRP3 inflammasome-derived IL18 and IL1β**

PBMCs were infected with Pru wild-type parasites and treated with either anti-IL12, anti-IL18, isotype specific antibody, or anti-IL12+anti-IL18 1 h p.i. Supernatants were harvested for quantification of IFNγ (**a**) and parasite growth (**b**). PBMCs were treated with the caspase 1/4 inhibitor VX765 or NLRP3 inhibitor MCC950 2 h pre-infection followed by infection for another 20 h. After harvesting the culture supernatant, IL1β (**c**), IL18 (**d**), IFNγ (**e**) and IL12/IL23p40 (**f**) were measured. Parasite growth was measured from the cell lysate using luciferase assay (**g**). Each dot represents the mean of 3 technical replicates from a single experiment. Statistical analysis was done with Two way ANOVA followed by Tukey's multiple comparison test (**a**), two sample Student's t test (**b and g**), and One way ANOVA followed by Tukey's multiple comparison test (**c-f**). Data are represented as mean ± standard error of the mean (SEM).

**Figure 5: Cytokine secretion from human PBMCs is mediated by activation of NFκB and p38 MAPK**

PBMCs were treated with indicated inhibitors 2 h prior to infection and subsequently infected for 20 h, after which IL12/IL23p40 (**a**), IL1β (**b**) and IFNγ were measured. The relative parasite growth was measured by luciferase growth assay (**d**). Each dot represents the mean of 3 technical replicates from an experiment. Statistical analysis

was done with One way ANOVA followed by Tukey's multiple comparison test. Data are represented as mean ± standard error of the mean (SEM).

**Figure 6: GRA15 and GRA24 induce cytokine secretion by human PBMCs**

PBMCs were infected with indicated *Toxoplasma* strains for 24 h, after which IL12/IL23p40 (**a**), IFNγ (**b**), TNFα (**c**), IL1β (**d**) were measured. Each dot represents the mean of 3 technical replicates from an experiment. Statistical analysis was done with One way ANOVA followed by Tukey's multiple comparison test. Data are represented as mean ± standard error of the mean (SEM).

**Supplementary Figure 1: Generation of knockout strains**

Sequence of the Hypoxanthine-guanine phosphoribosyltransferase (*HPT*) gene showing the sgDNA sequence in red for Cas9-mediated disruption and primer sequence in yellow (**a**). Disruption of the *HPT gene* was determined by using specific primers designed to amplify the region shown in the bottom figure, while *GRA27* was used as a housekeeping PCR control (at the top) (**b**). Schematic diagram of the strategy followed to delete *GRA24* (top) and PCR to screen the clones confirming the disruption of the gene (P1+P2) (bottom) is shown in (**c**). wild-type (left) and the presence of the insertion of the repair template in the locus (P1+P3) (right). Identification of Δ*gra24* and Δ*gra15/24* double knockout using specific primer sets for *GRA24* (top panel), *GRA15* (middle panel) and *GRA27* as a control for quality of the input DNA (lower panel) (**d**). Nuclear translocation of the p65 subunit of NFκB was quantified from infected RAW 264.7 macrophages 18 h p.i. with indicated strains. At least 15 cells were quantified as shown in the graph (left) and representative images are shown on the right (**e**).

Phenotypic confirmation of single clones of wild-type, Δ*gra15*, Δ*gra24* and Δ*gra15/24* parasites by their ability to activate NFκB (**f,g**) and p38 MAPK (**h**). Each dot represents the mean value of at least 15 host cell nuclei (**f and h**) or 3 technical replicates (**g**) from a single experiment. Statistical analysis was done by One way ANOVA followed by Tukey's multiple comparison test. Data are represented as mean ± standard error of the mean (SEM).

**Supplementary Figure 2:**

Mouse breeding scheme to generate in house *TLR11* knockout mice by cross-breeding homozygous $Tlr11^{-/-}$ male with homozygous $Tlr11^{+/+}$ female mice (**a**). Primers in the TLR11 locus (top) and PCR of the F1 progeny (bottom) where the homozygous $Tlr11^{+/+}$ yields a single band around 700 bp, homozygous $Tlr11^{-/-}$ generates a single band around 900 bp and all heterozygous mice generate both the bands at 700 bp and 900 bp (**b**).

**Supplementary Figure 3: Effect of GRA15 and GRA24 on cREL nuclear translocation**

Indicated parasite strains were added (MOI of 3) to confluent monolayers of HFFs grown on coverslips in 24-well plates. 16 h p.i. cells were fixed and stained with cREL antibody. Each dot represents the mean value of at least 15 host cell nuclei from a single experiment. A representative image for each group is shown on the right. Scale bar represents 10 µm. All the data are shown as mean ± SEM. Statistical analysis was done by two sample Student's t test.

**Supplementary Figure 4:**

*Tlr11*$^{-/-}$ mice were i.p infected with 5,000 tachyzoites of indicated *Toxoplasma* strains and 1 day p.i. serum was collected from each of the groups to measure IL12/IL23p40 (**a**). Survival and body weight measurements of *Tlr11*$^{-/-}$ mice (N=8 mice per group) that were i.p infected with 100-1000 tachyzoites (**b-c**) or 10 tissue cysts (**d-e**) of the indicated strains. *Tlr11*$^{-/-}$ mice were i.p injected with indicated doses of tachyzoites of different *Toxoplasma* strains derived from F1 progenies of type II X type III crosses (51) and body weight was measured daily throughout the infection (**f-h**). All the data are represented as mean ± SEM. Statistical analysis was done by two sample Student's t test and log rank test for survival curve.

**Supplementary Figure 5**

PMA differentiated THP1 macrophages were infected with indicated strains for 24 h and immunofluorescence assay was performed to quantify nuclear translocation of the NFκB p65 subunit (**a**), p-p38 MAPK (**b**) and NFκB cREL subunit (**c**). Scale bar represents 10 µm.

**Supplementary Figure 6:**

PBMCs or HFFs were infected with indicated *Toxoplasma* strains at three different MOIs for 24 h, after which supernatants were collected to measure S100A11 in PBMCs (**a**) and the PBMC lysates were used to measure parasite growth (**b**). S100A11 was measured in HFFs (**c**). Caspase 1/4 activity assay was measured from HFFs as described in materials and methods (**d**). Each dot represents the mean value of 3 technical replicates performed for each experiment. Statistical analysis was performed

706 by One way ANOVA followed by Tukey's multiple comparison test. Data are
707 represented as mean ± standard error of the mean (SEM).

708 **Acknowledgements**

709 This study was supported by the National Institutes of Health (R01-AI080621) awarded
710 to J.P.J.S. DM was supported by the American Heart Association Post-doctoral
711 fellowship (18POST34030036)

712

713 **References**

714 1. Sullivan WJ Jr, Jeffers V. 2012. Mechanisms of Toxoplasma gondii persistence and
715 latency. FEMS Microbiol Rev 36:717–733.

716 2. Dubey JP, Lindsay DS, Speer CA. 1998. Structures of Toxoplasma gondii
717 tachyzoites, bradyzoites, and sporozoites and biology and development of tissue
718 cysts. Clin Microbiol Rev 11:267–299.

719 3. Montoya JG, Liesenfeld O. 2004. Toxoplasmosis. Lancet 363:1965–1976.

720 4. Yarovinsky F. 2005. TLR11 Activation of Dendritic Cells by a Protozoan Profilin-Like
721 Protein. Science 308:1626–1629.

722 5. Koblansky AA, Jankovic D, Oh H, Hieny S, Sungnak W, Mathur R, Hayden MS,
723 Akira S, Sher A, Ghosh S. 2013. Recognition of profilin by Toll-like receptor 12 is
724 critical for host resistance to Toxoplasma gondii. Immunity 38:119–130.

725 6. Raetz M, Kibardin A, Sturge CR, Pifer R, Li H, Burstein E, Ozato K, Larin S,

726 Yarovinsky F. 2013. Cooperation of TLR12 and TLR11 in the IRF8-Dependent IL-12
727 Response to Toxoplasma gondii Profilin. The Journal of Immunology 191:4818 LP–
728 4827.

729 7. Yarovinsky F. 2014. Innate immunity to Toxoplasma gondii infection. Nat Rev
730 Immunol 14:109-121.

731 8. Trinchieri G. 2003. Interleukin-12 and the regulation of innate resistance and
732 adaptive immunity. Nat Rev Immunol 3:133–146.

733 9. Howard JC, Hunn JP, Steinfeldt T. 2011. The IRG protein-based resistance
734 mechanism in mice and its relation to virulence in Toxoplasma gondii. Curr Opin
735 Microbiol 14:414–421.

736 10. Niedelman W, Gold DA, Rosowski EE, Sprokholt JK, Lim D, Arenas AF, Melo MB,
737 Spooner E, Yaffe MB, Saeij JPJ. 2012. The rhoptry proteins ROP18 and ROP5
738 mediate Toxoplasma gondii evasion of the murine, but not the human, interferon-
739 gamma response. PLoS Pathog 8:e1002784.

740 11. Zhao YO, Khaminets A, Hunn JP, Howard JC. 2009. Disruption of the Toxoplasma
741 gondii parasitophorous vacuole by IFNγ-inducible immunity-related GTPases (IRG
742 proteins) triggers necrotic cell death. PLoS Pathog 5:e1000288.

743 12. Broz P, Dixit VM. 2016. Inflammasomes: Mechanism of assembly, regulation and
744 signalling. Nat Rev Immunol 16:407–420.

745 13. Gorfu G, Cirelli KM, Melo MB, Mayer-Barber K, Crown D, Koller BH, Masters S,
746 Sher A, Leppla SH, Moayeri M, Saeij JPJ, Grigg ME. 2014. Dual Role for

747 Inflammasome Sensors NLRP1 and NLRP3 in Murine Resistance to Toxoplasma
748 gondii. mBio 5:e01117-13.

749 14. Cai G, Kastelein R, Hunter CA. 2000. Interleukin-18 (IL-18) enhances innate IL-12-
750 mediated resistance to Toxoplasma gondii. Infect Immun 68:6932–6938.

751 15. Hunter CA, Chizzonite R, Remington JS. 1995. IL-1 beta is required for IL-12 to
752 induce production of IFN-gamma by NK cells. A role for IL-1 beta in the T cell-
753 independent mechanism of resistance against intracellular pathogens. J Immunol
754 155:4347–4354.

755 16. Yarovinsky F, Hieny S, Sher A. 2008. Recognition of Toxoplasma gondii by TLR11
756 prevents parasite-induced immunopathology. J Immunol 181:8478–8484.

757 17. Gazzinelli RT, Mendonça-Neto R, Lilue J, Howard J, Sher A. 2014. Innate
758 resistance against Toxoplasma gondii: an evolutionary tale of mice, cats, and men.
759 Cell Host Microbe 15:132–138.

760 18. Safronova A, Araujo A, Camanzo ET, Moon TJ, Elliott MR, Beiting DP, Yarovinsky
761 F. 2018. Alarmin S100A11 initiates a chemokine response to the human pathogen
762 Toxoplasma gondii. Nat Immunol 20:64-72.

763 19. Witola WH, Mui E, Hargrave A, Liu S, Hypolite M, Montpetit A, Cavailles P, Bisanz
764 C, Cesbron-Delauw MF, Fournié GJ, McLeod R. 2011. NALP1 influences
765 susceptibility to human congenital toxoplasmosis, proinflammatory cytokine
766 response, and fate of Toxoplasma gondii-infected monocytic cells. Infect Immun
767 79:756–766.

768 20. Gov L, Schneider CA, Lima TS, Pandori W, Lodoen MB. 2017. NLRP3 and
769 Potassium Efflux Drive Rapid IL-1β Release from Primary Human Monocytes during
770 Toxoplasma gondii Infection. The Journal of Immunology 199:2855 LP–2864.

771 21. Fisch D, Bando H, Clough B, Hornung V, Yamamoto M, Shenoy AR, Frickel E-M.
772 2019. Human GBP1 is a microbe-specific gatekeeper of macrophage apoptosis and
773 pyroptosis. EMBO J 38:e100926.

774 22. Hakimi M-A, Olias P, Sibley LD. 2017. Toxoplasma Effectors Targeting Host
775 Signaling and Transcription. Clin Microbiol Rev 30:615–645.

776 23. Hunter CA, Sibley LD. 2012. Modulation of innate immunity by Toxoplasma gondii
777 virulence effectors. Nat Rev Microbiol 10:766–778.

778 24. Lorenzi H, Khan A, Behnke MS, Namasivayam S, Swapna LS, Hadjithomas M,
779 Karamycheva S, Pinney D, Brunk BP, Ajioka JW, Ajzenberg D, Boothroyd JC,
780 Boyle JP, Dardé ML, Diaz-Miranda MA, Dubey JP, Fritz HM, Gennari SM, Gregory
781 BD, Kim K, Saeij JPJJ, Su C, White MW, Zhu XQ, Howe DK, Rosenthal BM, Grigg
782 ME, Parkinson J, Liu L, Kissinger JC, Roos DS, Sibley LD. 2016. Local admixture of
783 amplified and diversified secreted pathogenesis determinants shapes mosaic
784 Toxoplasma gondii genomes. Nat Commun 7:10147.

785 25. Saeij JPJ, Boyle JP, Boothroyd JC. 2005. Differences among the three major
786 strains of Toxoplasma gondii and their specific interactions with the infected host.
787 Trends Parasitol 21:476–481.

788 26. Ajzenberg D, Cogné N, Paris L, Bessières M, Thulliez P, Filisetti D, Pelloux H,

789 Marty P, Dardé M. 2002. Genotype of 86Toxoplasma gondiiIsolates Associated with
790 Human Congenital Toxoplasmosis, and Correlation with Clinical Findings. The
791 Journal of Infectious Diseases 186:684-689.

792 27. Behnke MS, Khan A, Lauron EJ, Jimah JR, Wang Q, Tolia NH, Sibley LD. 2015.
793 Rhoptry Proteins ROP5 and ROP18 Are Major Murine Virulence Factors in
794 Genetically Divergent South American Strains of Toxoplasma gondii. PLoS Genet
795 11:e1005434.

796 28. Fleckenstein MC, Reese ML, Konen-Waisman S, Boothroyd JC, Howard JC,
797 Steinfeldt T. 2012. A Toxoplasma gondii pseudokinase inhibits host IRG resistance
798 proteins. PLoS Biol 10:e1001358.

799 29. Steinfeldt T, Konen-Waisman S, Tong L, Pawlowski N, Lamkemeyer T, Sibley LD,
800 Hunn JP, Howard JC. 2010. Phosphorylation of mouse immunity-related GTPase
801 (IRG) resistance proteins is an evasion strategy for virulent Toxoplasma gondii.
802 PLoS Biol 8:e1000576.

803 30. Alaganan A, Fentress SJ, Tang K, Wang Q, Sibley LD. 2014. Toxoplasma GRA7
804 effector increases turnover of immunity-related GTPases and contributes to acute
805 virulence in the mouse. Proc Natl Acad Sci U S A 111:1126–1131.

806 31. Rosowski EE, Lu D, Julien L, Rodda L, Gaiser RA, Jensen KDC, Saeij JPJ. 2011.
807 Strain-specific activation of the NF-κB pathway by GRA15, a novel *Toxoplasma*
808 *gondii* dense granule protein. J Exp Med 208:195–212.

809 32. Ma JS, Sasai M, Ohshima J, Lee Y, Bando H, Takeda K, Yamamoto M. 2014.

Selective and strain-specific NFAT4 activation by the *Toxoplasma gondii* polymorphic dense granule protein GRA6. J Exp Med 211:2013–2032.

33. Gov L, Karimzadeh A, Ueno N, Lodoen MB. 2013. Human innate immunity to Toxoplasma gondii is mediated by host caspase-1 and ASC and parasite GRA15. MBio 4:e00255-13.

34. Bougdour A, Durandau E, Brenier-Pinchart MP, Ortet P, Barakat M, Kieffer S, Curt-Varesano A, Curt-Bertini RL, Bastien O, Coute Y, Pelloux H, Hakimi MA. 2013. Host cell subversion by Toxoplasma GRA16, an exported dense granule protein that targets the host cell nucleus and alters gene expression. Cell Host Microbe 13:489–500.

35. Braun L, Brenier-Pinchart M-P, Yogavel M, Curt-Varesano A, Curt-Bertini R-L, Hussain T, Kieffer-Jaquinod S, Coute Y, Pelloux H, Tardieux I, Sharma A, Belrhali H, Bougdour A, Hakimi M-A. 2013. A *Toxoplasma* dense granule protein, GRA24, modulates the early immune response to infection by promoting a direct and sustained host p38 MAPK activation. J Exp Med 210:2071–2086.

36. Gay G, Braun L, Brenier-Pinchart M-P, Vollaire J, Josserand V, Bertini R-L, Varesano A, Touquet B, De Bock P-J, Coute Y, Tardieux I, Bougdour A, Hakimi M-A. 2016. *Toxoplasma gondii* TgIST co-opts host chromatin repressors dampening STAT1-dependent gene regulation and IFN-γ–mediated host defenses. J Exp Med 213:1779–1798.

37. Jensen KDC, Wang Y, Wojno EDT, Shastri AJ, Hu K, Cornel L, Boedec E, Ong Y-

C, Chien Y-H, Hunter CA, Boothroyd JC, Saeij JPJ. 2011. Toxoplasma Polymorphic Effectors Determine Macrophage Polarization and Intestinal Inflammation. Cell Host Microbe 9:472–483.

38. Murray PJ, Allen JE, Biswas SK, Fisher EA, Gilroy DW, Goerdt S, Gordon S, Hamilton JA, Ivashkiv LB, Lawrence T, Locati M, Mantovani A, Martinez FO, Mege J-L, Mosser DM, Natoli G, Saeij JP, Schultze JL, Shirey KA, Sica A, Suttles J, Udalova I, van Ginderachter JA, Vogel SN, Wynn TA. 2014. Macrophage Activation and Polarization: Nomenclature and Experimental Guidelines. Immunity 41:14–20.

39. Chen L, Christian DA, Kochanowsky JA, Phan AT, Clark JT, Wang S, Berry C, Oh J, Chen X, Roos DS, Beiting DP, Koshy AA, Hunter CA. 2020. The Toxoplasma gondii virulence factor ROP16 acts in cis and trans, and suppresses T cell responses. The Journal of Experimental Medicine 217: e20181757.

40. Butcher BA, Fox BA, Rommereim LM, Kim SG, Maurer KJ, Yarovinsky F, Herbert DR, Bzik DJ, Denkers EY. 2011. Toxoplasma gondii rhoptry kinase ROP16 activates STAT3 and STAT6 resulting in cytokine inhibition and arginase-1-dependent growth control. PLoS Pathog 7:e1002236.

41. Jensen KDC, Hu K, Whitmarsh RJ, Hassan MA, Julien L, Lu D, Chen L, Hunter CA, Saeij JPJ. 2013. Toxoplasma gondii rhoptry 16 kinase promotes host resistance to oral infection and intestinal inflammation only in the context of the dense granule protein GRA15. Infect Immun 81:2156–2167.

42. Sturge CR, Benson A, Raetz M, Wilhelm CL, Mirpuri J, Vitetta ES, Yarovinsky F.

852 2013. TLR-independent neutrophil-derived IFN- is important for host resistance to
853 intracellular pathogens. Proceedings of the National Academy of Sciences
854 110:10711-10716.

855 43. López-Yglesias AH, Camanzo E, Martin AT, Araujo AM, Yarovinsky F. 2019.
856 TLR11-independent inflammasome activation is critical for CD4+ T cell-derived IFN-
857 γ production and host resistance to Toxoplasma gondii. PLoS Pathog 15:e1007872.

858 44. Robben PM, Mordue DG, Truscott SM, Takeda K, Akira S, Sibley LD. 2004.
859 Production of IL-12 by Macrophages Infected with Toxoplasma gondii Depends on
860 the Parasite Genotype. The Journal of Immunology 172:3686–3694.

861 45. Kim L, Rio LD, Butcher BA, Mogensen TH, Paludan SR, Flavell RA, Denkers EY.
862 2005. p38 MAPK Autophosphorylation Drives Macrophage IL-12 Production during
863 Intracellular Infection. The Journal of Immunology 174:4178–4184.

864 46. Sanjabi S, Hoffmann A, Liou H-C, Baltimore D, Smale ST. 2000. Selective
865 requirement for c-Rel during IL-12 P40 gene induction in macrophages.
866 Proceedings of the National Academy of Sciences 97:12705–12710.

867 47. Reese ML, Zeiner GM, Saeij JPJ, Boothroyd JC, Boyle JP. 2011. Polymorphic
868 family of injected pseudokinases is paramount in Toxoplasma virulence. Proc Natl
869 Acad Sci U S A 108:9625–9630.

870 48. Saeij JPJ, Boyle JP, Coller S, Taylor S, Sibley LD, Brooke-Powell ET, Ajioka JW,
871 Boothroyd JC. 2006. Polymorphic secreted kinases are key virulence factors in
872 toxoplasmosis. Science 314:1780–1783.

873 49. Taylor S, Barragan A, Su C, Fux B, Fentress SJ, Tang K, Beatty WL, Hajj HE,
874 Jerome M, Behnke MS, White M, Wootton JC, Sibley LD. 2006. A secreted serine-
875 threonine kinase determines virulence in the eukaryotic pathogen Toxoplasma
876 gondii. Science 314:1776–1780.

877 50. Behnke MS, Fentress SJ, Mashayekhi M, Li LX, Taylor GA, Sibley LD. 2012. The
878 polymorphic pseudokinase ROP5 controls virulence in Toxoplasma gondii by
879 regulating the active kinase ROP18. PLoS Pathog 8:e1002992.

880 51. Sibley LD, LeBlanc AJ, Pfefferkorn ER, Boothroyd JC. 1992. Generation of a
881 restriction fragment length polymorphism linkage map for Toxoplasma gondii.
882 Genetics 132:1003–1015.

883 52. Selleck EM, Orchard RC, Lassen KG, Beatty WL, Xavier RJ, Levine B, Virgin HW,
884 Sibley LD. 2015. A Noncanonical Autophagy Pathway Restricts Toxoplasma gondii
885 Growth in a Strain-Specific Manner in IFN-gamma-Activated Human Cells. mBio
886 6:e01157–15.

887 53. Spiller KL, Wrona EA, Romero-Torres S, Pallotta I, Graney PL, Witherel CE,
888 Panicker LM, Feldman RA, Urbanska AM, Santambrogio L, Vunjak-Novakovic G,
889 Freytes DO. 2016. Differential gene expression in human, murine, and cell line-
890 derived macrophages upon polarization. Exp Cell Res 347:1–13.

891 54. Pierce JW, Schoenleber R, Jesmok G, Best J, Moore SA, Collins T, Gerritsen ME.
892 1997. Novel Inhibitors of Cytokine-induced IκBα Phosphorylation and Endothelial
893 Cell Adhesion Molecule Expression Show Anti-inflammatory Effects in Vivo. J Biol

894 Chem 272:21096–21103.

895 55. Pargellis C, Tong L, Churchill L, Cirillo PF, Gilmore T, Graham AG, Grob PM,
896 Hickey ER, Moss N, Pav S, Regan J. 2002. Inhibition of p38 MAP kinase by utilizing
897 a novel allosteric binding site. Nat Struct Biol 9:268–272.

898 56. Tosh KW, Mittereder L, Bonne-Annee S, Hieny S, Nutman TB, Singer SM, Sher A,
899 Jankovic D. 2016. The IL-12 Response of Primary Human Dendritic Cells and
900 Monocytes to *Toxoplasma gondii* Is Stimulated by Phagocytosis of Live Parasites
901 Rather Than Host Cell Invasion. The Journal of Immunology 196:345–356.

902 57. Andrade WA, Souza M do C, Ramos-Martinez E, Nagpal K, Dutra MS, Melo MB,
903 Bartholomeu DC, Ghosh S, Golenbock DT, Gazzinelli RT. 2013. Combined action
904 of nucleic acid-sensing Toll-like receptors and TLR11/TLR12 heterodimers imparts
905 resistance to Toxoplasma gondii in mice. Cell Host Microbe 13:42–53.

906 58. Sturge CR, Yarovinsky F. 2014. Complex immune cell interplay in the gamma
907 interferon response during Toxoplasma gondii infection. Infect Immun 82:3090–
908 3097.

909 59. Mashayekhi M, Sandau MM, Dunay IR, Frickel EM, Khan A, Goldszmid RS, Sher A,
910 Ploegh HL, Murphy TL, Sibley LD, Murphy KM. 2011. CD8α+ Dendritic Cells Are
911 the Critical Source of Interleukin-12 that Controls Acute Infection by Toxoplasma
912 gondii Tachyzoites. Immunity 35:249–259.

913 60. Schade B, Fischer HG. 2001. Toxoplasma gondii induction of interleukin-12 is
914 associated with acute virulence in mice and depends on the host genotype. Vet

915 Parasitol 100:63–74.

916 61. Scanga CA, Aliberti J, Jankovic D, Tilloy F, Bennouna S, Denkers EY, Medzhitov R,
917 Sher A. 2002. Cutting edge: MyD88 is required for resistance to Toxoplasma gondii
918 infection and regulates parasite-induced IL-12 production by dendritic cells. J
919 Immunol 168:5997–6001.

920 62. Aliberti J, Reis e Sousa C, Schito M, Hieny S, Wells T, Huffnagle GB, Sher A. 2000.
921 CCR5 provides a signal for microbial induced production of IL-12 by CD8α+
922 dendritic cells. Nat Immunol 1:83–87.

923 63. Grumont R, Hochrein H, O'Keeffe M, Gugasyan R, White C, Caminschi I, Cook W,
924 Gerondakis S. 2001. c-Rel regulates interleukin 12 p70 expression in CD8(+)
925 dendritic cells by specifically inducing p35 gene transcription. J Exp Med 194:1021–
926 1032.

927 64. Melo MB, Nguyen QP, Cordeiro C, Hassan MA, Yang N, McKell R, Rosowski EE,
928 Julien L, Butty V, Dardé ML, Ajzenberg D, Fitzgerald K, Young LH, Saeij JPJ. 2013.
929 Transcriptional Analysis of Murine Macrophages Infected with Different Toxoplasma
930 Strains Identifies Novel Regulation of Host Signaling Pathways. PLoS Pathog 9:
931 e1003779 .

932 65. Morgado P, Sudarshana DM, Gov L, Harker KS, Lam T, Casali P, Boyle JP, Lodoen
933 MB. 2014. Type II Toxoplasma gondii induction of CD40 on infected macrophages
934 enhances interleukin-12 responses. Infect Immun 82:4047–4055.

935 66. Song J, Wilhelm CL, Wangdi T, Maira-Litran T, Lee S-J, Raetz M, Sturge CR,

936 Mirpuri J, Pei J, Grishin NV, McSorley SJ, Gewirtz AT, Baumler AJ, Pier GB, Galan
937 JE, Yarovinsky F. 2016. Absence of TLR11 in Mice Does Not Confer Susceptibility
938 to Salmonella Typhi. Cell 164:827-828.

939 67. Johnson AM. 1984. Strain-dependent, route of challenge-dependent, murine
940 susceptibility to toxoplasmosis. Z Parasitenkd 70:303–309.

941 68. Acosta Davila JA, Hernandez De Los Rios A. 2019. An Overview of Peripheral
942 Blood Mononuclear Cells as a Model for Immunological Research of Toxoplasma
943 gondii and Other Apicomplexan Parasites. Front Cell Infect Microbiol 9:24.

944 69. Autissier P, Soulas C, Burdo TH, Williams KC. 2010. Evaluation of a 12-color flow
945 cytometry panel to study lymphocyte, monocyte, and dendritic cell subsets in
946 humans. Cytometry A 77:410–419.

947 70. Berenson LS, Yang J, Sleckman BP, Murphy TL, Murphy KM. 2006. Selective
948 Requirement of p38α MAPK in Cytokine-Dependent, but Not Antigen Receptor-
949 Dependent, Th1 Responses. The Journal of Immunology 176:4616–4621.

950 71. Zhao Y, Marple AH, Ferguson DJP, Bzik DJ, Yap GS. 2014. Avirulent strains of
951 Toxoplasma gondii infect macrophages by active invasion from the phagosome.
952 Proceedings of the National Academy of Sciences 111:6437–6442.

953 72. Channon JY, Seguin RM, Kasper LH. 2000. Differential Infectivity and Division of
954 Toxoplasma gondii in Human Peripheral Blood Leukocytes. Infect Immun 68:4822–
955 4826.

956 73. Gaidt MM, Ebert TS, Chauhan D, Schmidt T, Schmid-Burgk JL, Rapino F,

957 Robertson AAB, Cooper MA, Graf T, Hornung V. 2016. Human Monocytes Engage
958 an Alternative Inflammasome Pathway. Immunity 44:833–846.

959 74. Mukhopadhyay D, Saeij JPJ. 2020. Assays to Evaluate Toxoplasma-Macrophage
960 Interactions. Methods Mol Biol 2071:347–370.

961 75. Kim S-K, Karasov A, Boothroyd JC. 2007. Bradyzoite-Specific Surface Antigen
962 SRS9 Plays a Role in Maintaining Toxoplasma gondii Persistence in the Brain and
963 in Host Control of Parasite Replication in the Intestine. Infect Immun 75:1626 LP–
964 1634.

965 76. Fox BA, Falla A, Rommereim LM, Tomita T, Gigley JP, Mercier C, Cesbron-Delauw
966 M-F, Weiss LM, Bzik DJ. 2011. Type II Toxoplasma gondii KU80 knockout strains
967 enable functional analysis of genes required for cyst development and latent
968 infection. Eukaryot Cell 10:1193–1206.

969 77. Wang Y, Cirelli KM, Barros PDC, Sangaré LO, Butty V, Hassan MA, Pesavento P,
970 Mete A, Saeij JPJ. 2019. Three Toxoplasma gondii Dense Granule Proteins Are
971 Required for Induction of Lewis Rat Macrophage Pyroptosis. mBio 10:e02388–18.

972 78. Heaslip AT, Nishi M, Stein B, Hu K. 2011. The Motility of a Human Parasite,
973 Toxoplasma gondii, Is Regulated by a Novel Lysine Methyltransferase. PLoS
974 Pathog 7:e1002201.

975 79. Mukhopadhyay D, Mukherjee S, Roy S, Dalton JE, Kundu S, Sarkar A, Das NK,
976 Kaye PM, Chatterjee M. 2015. M2 Polarization of Monocytes-Macrophages Is a
977 Hallmark of Indian Post Kala-Azar Dermal Leishmaniasis. PLoS Negl Trop Dis

978 9:e0004145.

979 **Primer and sgRNA sequences (Table 1)**

| Name | Sequence |
|---|---|
| TGME49_200320_gRNA1_Fwd | 5’ AAGTT **GACAAAATCCTCCTCCCTGG** G 3’ |
| TGME49_200320_gRNA1_Rev | 5’ AAAAC **CCAGGGAGGAGGATTTTGTC** A 3’ |
| TGME49_200320_gRNA2_Fwd | 5’ AAGTT **GGACATAGTGCTCGAAGAAG** G 3’ |
| TGME49_200320_gRNA2_Rev | 5’ AAAAC **CTTCTTCGAGCACTATGTCC** A 3 |
| TGME49_230180_gRNA1_Fwd | 5’ AAGTT **GTACCAGGCTACAAATAGAGA** G 3’ |
| TGME49_230180_gRNA1_Rev | 5’ AAAAC **TCTCTATTTGTAGCCTGGTAC**A 3’ |
| TGME49_230180_gRNA2_Fwd | 5’ AAGTT**GGGACCGAAATGCCGAATCA** G 3’ |
| TGME49_230180_gRNA2_Rev | 5’ AAAAC**TGATTCGGCATTTCGGTCCC** A 3 |
| HPT_Fwd | 5’ ATGGCGTCCAAACCCATTGA 3’ |
| HPT_Rev | 5’ TCGTTGAAGTCGTAGCAGCA 3’ |
| GRA24_Fwd | 5**’** ATGCTCCAGATGGCACGATATACCG 3’ |
| GRA24_Rev | 5’ CTGTCGTCTGCTGGTGGTAGC 3’ |
| DHFR_Rev | 5’ ATAGTCCTGTCGGGTTTCGCCAC 3’ |
| GRA15_Fwd | 5**’** AACACGACGAGGCAGGAGAATTAC 3’ |
| GRA15_Rev | 5’ GACGACTGTAGCCTGAGCATCC 3’ |

| | |
|---|---|
| Neo74 | 5’ GTGGGATTAGATAAATGCCTGCTC 3’ |
| 5ARMF2 | 5’ AACACAGGCTCAGAAGAGAAGAGG 3’ |
| 2285 | 5’ TTGATGTATTCGTGTCCCACTGC 3’ |
| +3AMR | 5’ GCGGACACCTTCCATCTCTCAGTT 3’ |

980

981 Nucleotides highlighted in grey are part of the *BsaI* cloning site of pSS013 and

982 nucleotides in bold are the actual sgDNA sequence.

Figure 1

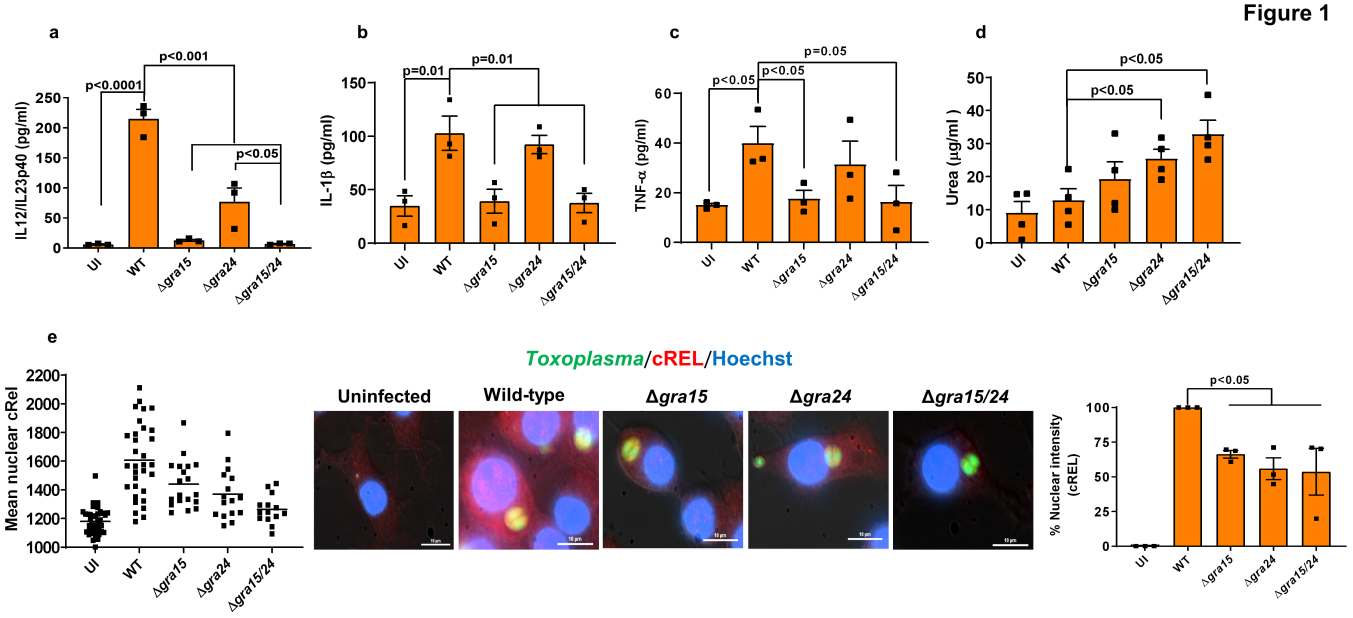


**Figure 1: GRA15 and GRA24 activate the *in vitro* macrophage response**

BMDMs were infected with indicated *Toxoplasma* strains for 24 h and IL12/IL23p40 (**a**), IL1β (**b**) and TNFα (**c**) were measured in the supernatant. Experiments were done 3 times. Arginase activity was measured (**d**) from RAW 264.7 macrophages infected with indicated strains 24 h p.i. Nuclear translocation of the cREL subunit of NFκB (**e**) was quantified from infected RAW 264.7 macrophages 18 h p.i. with indicated strains. In each experiment at least 15 cells were quantified as shown in the graph (left) and experiment was done 3 times (right panel graph). A representative image for each group is shown in the middle panel. Scale bar is 10 µm. Each dot represents the mean of 3 technical replicates from individual experiments, except for the scatter diagram in (e). Statistical analysis was done by two sample student's t test for figures a-e. Data are represented as mean ± standard error of the mean (SEM).

Figure 2

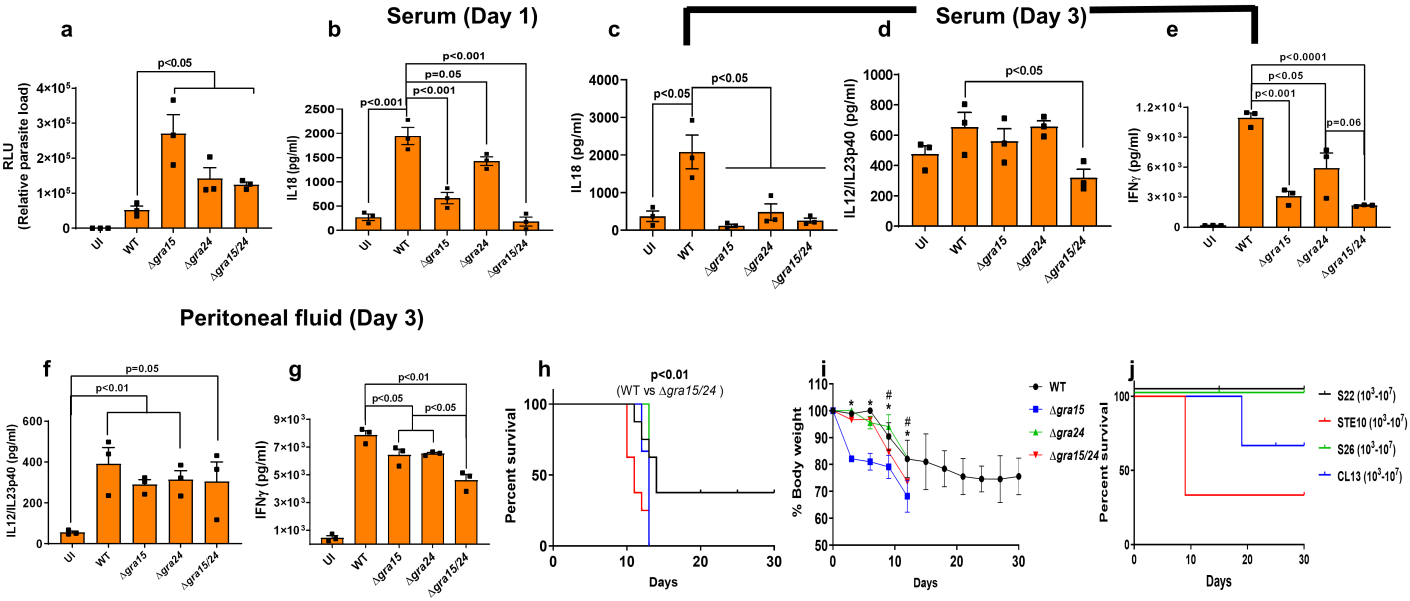


**Figure 2: Deletion of *GRA15* and *GRA24* leads to enhanced parasite virulence in *Tlr11*$^{-/-}$ mice**

*Tlr11*$^{-/-}$ mice were i.p. infected with 5,000 tachyzoites of indicated *Toxoplasma* strains expressing luciferase, and serum and peritoneal fluid were collected from each mouse (N=3 mice per group) at different time points. (**a**) Three days p.i. peritoneal cells were isolated, plated in tissue culture plates for 24 h and the following day luciferase reading was taken to measure the parasite burden. (**b**) Serum IL18 levels at 1 day p.i. Serum IL18 (**c**), IL12/IL23p40 (**d**) and IFNγ (**e**) levels 3 days p.i.. IL12/IL23p40 (**f**) and IFNγ (**g**) levels in the peritoneal fluid 3 days p.i. All data represent mean ± SEM. Statistical analysis was done with two sample Student's t tests. *Tlr11*$^{-/-}$ mice were s.c. infected with 5,000 tachyzoites of indicated strains and (**h**) survival and (**i**) weight (plotted as an average of the change in body weight for each cohort, where 100% body weight corresponds to the day of infection) of the mice were monitored for 30 days. Statistical analysis was done using a log-rank test. N=8 each for wild-type and Δ*gra15/24* whereas N=5 for Δ*gra15* and Δ*gra24*. *Tlr11*$^{-/-}$ mice were i.p injected with indicated doses of tachyzoites of different *Toxoplasma* strains derived from F1 progenies of a type II X type III cross (51) containing avirulent *ROP18* and *ROP5* alleles and survival was monitored (**j**). Each dot represents a mean of 3 technical replicates from an experiment. Statistical analysis was done by two sample student's t test for figures a-g. Data are represented as mean ± standard error of the mean (SEM).

**Figure 3**

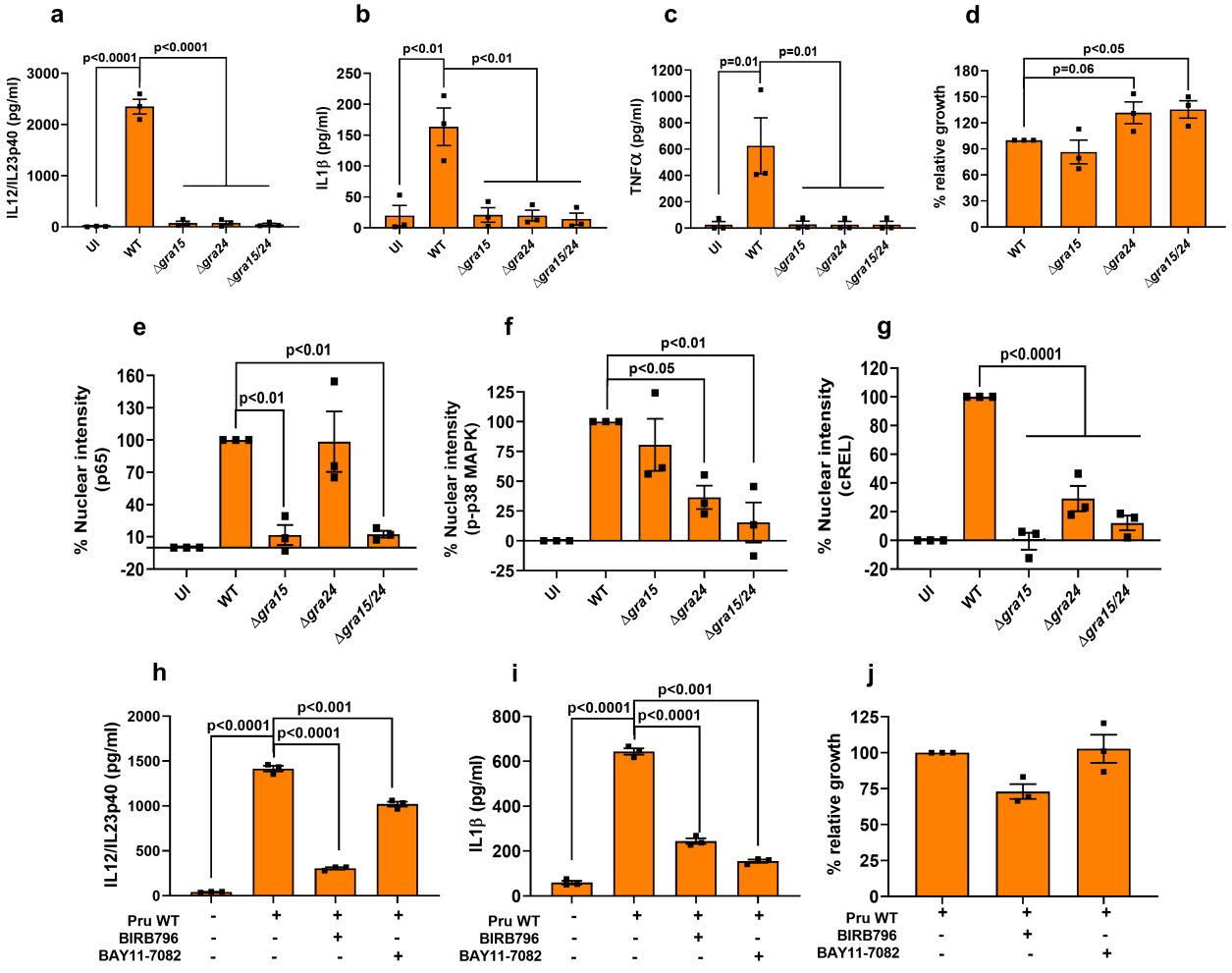


**Figure 3: GRA15 and GRA24 activate pro-inflammatory cytokine secretion by human macrophages.**

THP1 monocyte-derived macrophages were infected with indicated *Toxoplasma* strains for 24 h, after which IL12/IL23p40 (**a**), IL1β (**b**) and TNFα were measured. Relative parasite growth was measured by luciferase growth assay (**d**). Nuclear translocation of the NFκB p65 (**e**), p-p38 MAPK (**f**), and NFκB cREL (**g**) subunits were quantified from infected THP1 macrophages 18 h p.i with indicated strains. In each experiment at least 15 cells were quantified. THP1 macrophages were treated with indicated inhibitors 2 h prior to infection and subsequently infected for an additional 20 h. IL12/IL23p40 (**h**), IL1β (**i**) and growth (**j**) were measured. Each dot represents a technical mean value from a single experiment, and each experiment was done 3 times. Statistical analysis was done by One way ANOVA followed with Tukey's multiple comparison test. Data are represented as mean ± standard error of the mean (SEM).

Figure 4

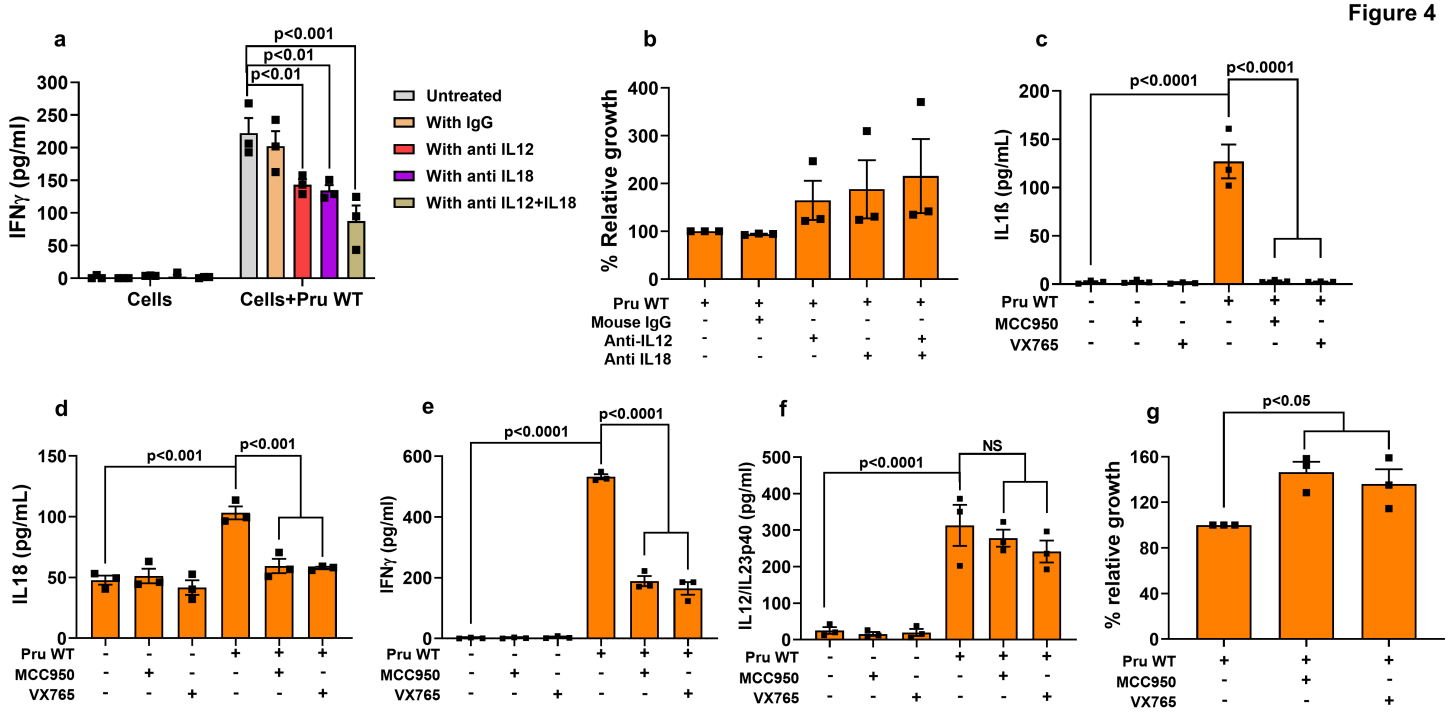


**Figure 4: Secretion of IFNγ from human PBMCs is dependent on IL12 and NLRP3 inflammasome-derived IL18 and IL1β**

PBMCs were infected with Pru wild-type parasites and treated with either anti-IL12, anti-IL18, isotype specific antibody, or anti-IL12+anti-IL18 1 h p.i. Supernatants were harvested for quantification of IFNγ (**a**) and parasite growth (**b**). PBMCs were treated with the caspase 1/4 inhibitor VX765 or NLRP3 inhibitor MCC950 2 h pre-infection followed by infection for another 20 h. After harvesting the culture supernatant, IL1β (**c**), IL18 (**d**), IFNγ (**e**) and IL12/IL23p40 (**f**) were measured. Parasite growth was measured from the cell lysate using luciferase assay (**g**). Each dot represents the mean of 3 technical replicates from a single experiment. Statistical analysis was done with Two way ANOVA followed by Tukey's multiple comparison test (**a**), two sample Student's t test (**b and g**), and One way ANOVA followed by Tukey's multiple comparison test (**c-f**). Data are represented as mean ± standard error of the mean (SEM).

**Figure 5**

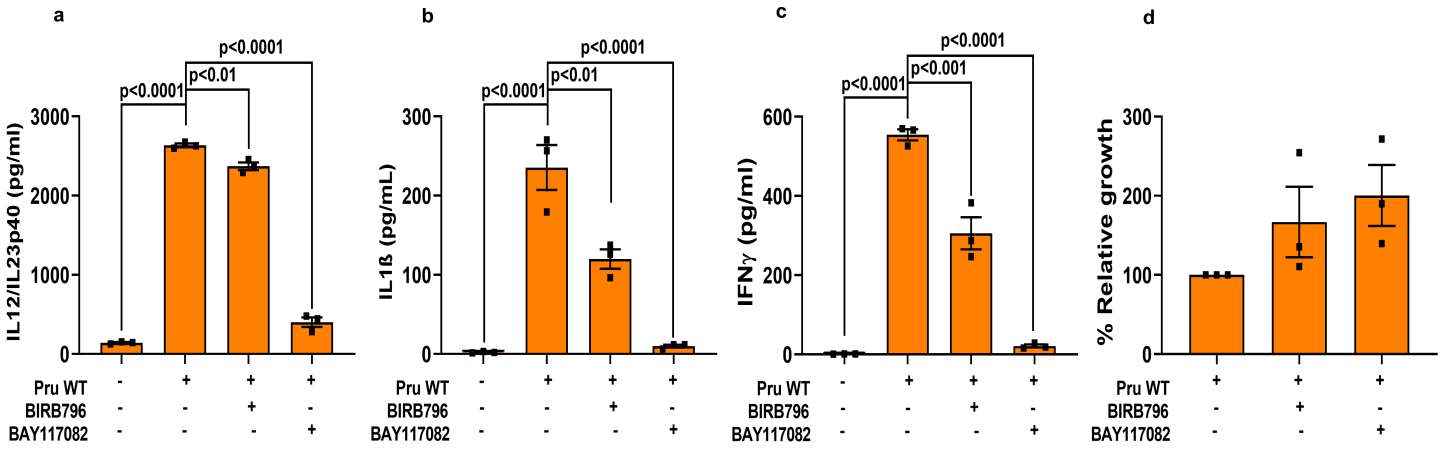


**Figure 5: Cytokine secretion from human PBMCs is mediated by activation of NFκB and p38 MAPK**

PBMCs were treated with indicated inhibitors 2 h prior to infection and subsequently infected for 20 h, after which IL12/IL23p40 (**a**), IL1β (**b**) and IFNγ were measured. The relative parasite growth was measured by luciferase growth assay (**d**). Each dot represents the mean of 3 technical replicates from an experiment. Statistical analysis was done with One way ANOVA followed by Tukey's multiple comparison test. Data are represented as mean ± standard error of the mean (SEM).

**Figure 6**

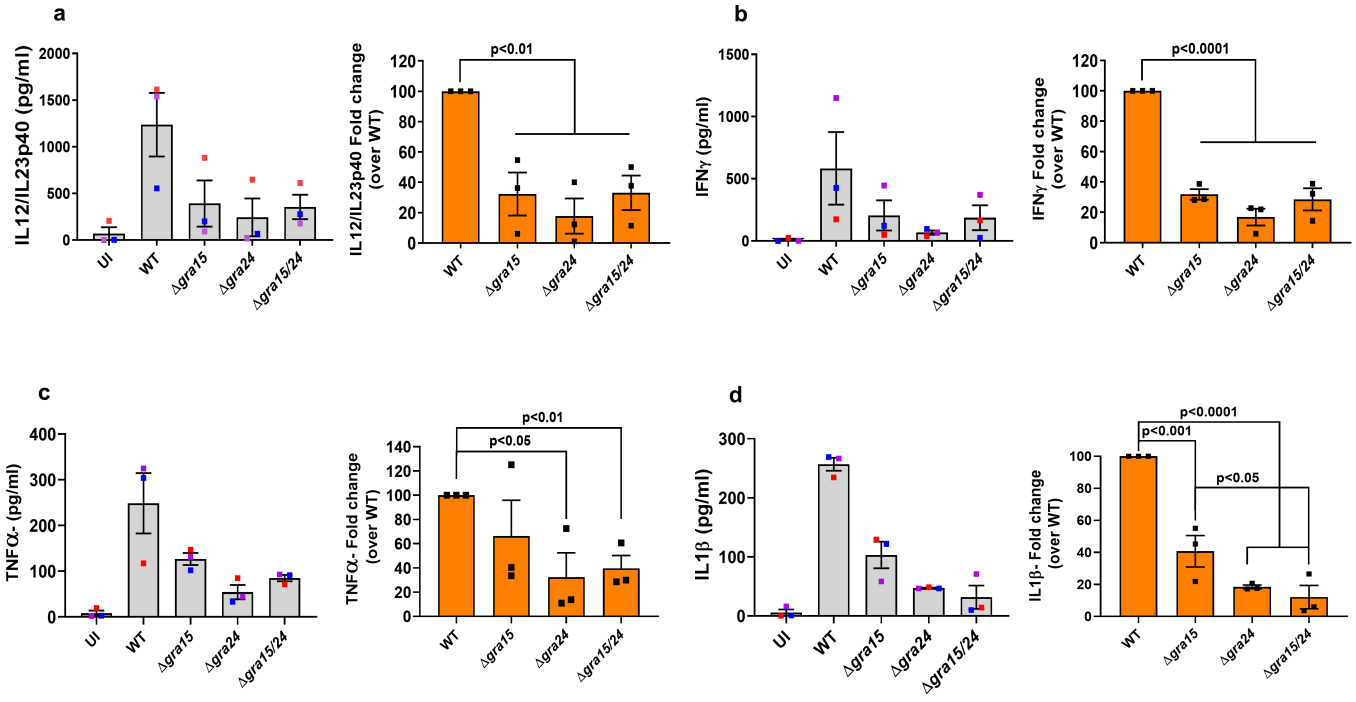


**Figure 6: GRA15 and GRA24 induce cytokine secretion by human PBMCs**

PBMCs were infected with indicated *Toxoplasma* strains for 24 h, after which IL12/IL23p40 (**a**), IFNγ (**b**), TNFα (**c**), IL1β (**d**) were measured. Each dot represents the mean of 3 technical replicates from an experiment. Statistical analysis was done with One way ANOVA followed by Tukey's multiple comparison test. Data are represented as mean ± standard error of the mean (SEM).